AD621145

AFWL-TR-65-99

AFWL-TR
65-99

# BEHAVIOR OF FLEXIBLE UNDERGROUND CYLINDERS

Ulrich Luscher

Massachusetts Institute of Technology
Department of Civil Engineering
Cambridge, Massachusetts

Contract AF 29(601)-6368

TECHNICAL REPORT NO. AFWL-TR-65-99

September 1965

CLEARINGHOUSE
FOR FEDERAL SCIENTIFIC AND
TECHNICAL INFORMATION
Hardcopy | Microfiche
$3.00 | $0.75 | 73 as
ARCHIVE

AIR FORCE WEAPONS LABORATORY
Research and Technology Division
Air Force Systems Command
Kirtland Air Force Base
New Mexico

DDC
SEP 28 1965
DDC-IRA E

AFWL TR-65-99

# BEHAVIOR OF FLEXIBLE UNDERGROUND CYLINDERS

Ulrich Luscher

Massachusetts Institute of Technology
Department of Civil Engineering
Cambridge, Massachusetts
Contract AF 29(601)-6368

# FOREWORD

This is one of two reports describing the research conducted at the Massachusetts Institute of Technology, Cambridge, Massachusetts, under Contract AF 29(601)-6368 with the Air Force Weapons Laboratory (AFWL) between 1 March 1964 and 2 April 1965. Lieutenant J. A. Eddings, AFWL (WLDC), was the project officer for the Air Force. The research was funded under DASA Project 5710, Subtask 13.157, Program Element 7.60.06.01.D. The report was submitted 10 August 1965. This work represents a logical continuation of the small-scale soil-structure interaction studies undertaken previously at M.I.T. and reported in the following reports and publications: Whitman, Luscher, and Philippe (1961); Whitman and Luscher (1962); Luscher (1963); Luscher and Höeg (1964a); Luscher and Höeg (1964b).

The research was performed in the Soil Research Laboratories of the Department of Civil Engineering at M.I.T. The Head of the Soils Laboratories and general supervisor of the project was Dr. T. W. Lambe, Professor of Civil Engineering. Dr. R. V. Whitman, Professor of Civil Engineering, contributed many valuable suggestions. Dr. U. Luscher, Assistant Professor of Civil Engineering, was Principal Investigator under this contract. This report was prepared by Dr. Luscher.

This technical report has been reviewed and is approved.

James A. Eddings

JAMES A. EDDINGS
1Lt USAF
Project Officer

Robert E. Crawford

ROBERT E. CRAWFORD
Major USAF
Deputy Chief, Civil
Engineering Branch

John W. Kodis

JOHN W. KODIS
Colonel USAF
Chief, Development
Division

## ABSTRACT

An investigation was made of the "elastic" behavior and failure condition of underground flexible cylinders with particular attention given to arching, deformation and buckling. The report presents no new data, rather draws heavily from experimental and theoretical work done in the past several years in an attempt to arrive at a unified picture of the chosen aspects of behavior. Active arching was found to reduce the load acting on tubes buried at depths up to several diameters in stiff soil by an average of 30 percent. On the other hand, passive arching may subject tubes buried in compressible soil to loads somewhat higher than applied on the surface. Spangler's deformation equation was modified to account for arching, lateral pressures, and variability of the soil modulus with pressure. Values of the modified modulus of passive soil resistance, backcalculated by the new equation from tube deformation data, were successfully related to the constrained modulus of the soil. A comprehensive theory of buckling of underground cylinders is presented. It starts with the previously derived theory for elastic buckling in the circular-symmetric tube-soil configuration and extends it to cover (1) elastic buckling of an underground cylinder; (2) inelastic buckling; (3) the effects of soil stiffness and presence of water; and (4) buckling of corrugated cylinders. It proved possible to correlate the soil modulus $K_s$ controlling buckling to the constrained modulus M of the soil. The theory agreed well with the few available data. More comparisons with laboratory and field data are required, in particular to verify the values of $K_s$ and their relationship to values of M. Regardless of the exact value of $K_s$, however, it was shown that for many practical situations of underground cylinders the controlling mode of failure is buckling rather than compressive yield.

BLANK PAGE

CONTENTS


| | | Page |
|---|---|---|
| Chapter 1 | INTRODUCTION | 1 |
| Chapter 2 | BASIC CONCEPTS OF BEHAVIOR OF FLEXIBLE CYLINDERS | 5 |
| 2.1 | Introduction | 5 |
| 2.2 | Arching | 6 |
| 2.3 | Deformation of Flexible Cylinders | 10 |
| 2.4 | Failure of Flexible Cylinders | 23 |
| Chapter 3 | BUCKLING OF FLEXIBLE UNDERGROUND CYLINDERS | 27 |
| 3.1 | Introduction | 27 |
| 3.2 | Elastic Buckling of Soil-Surrounded, Smooth Cylinders | 27 |
| 3.3 | Inelastic Buckling of Soil-Surrounded, Smooth Cylinders | 35 |
| 3.4 | Buckling of Fully Buried Cylinders | 38 |
| 3.5 | Buckling of Shallow-Buried Cylinders | 42 |
| 3.6 | Buckling Resistance of Corrugated Cylinders | 46 |
| 3.7 | Effect of Soil Stiffness and Pore Pressure on Tube Buckling Resistance | 48 |
| Chapter 4 | SUMMARY AND CONCLUSIONS | 55 |
| 4.1 | Summary | 55 |
| 4.2 | Conclusions Regarding the Importance of Tube Buckling | 58 |
| REFERENCES | | 59 |
| DISTRIBUTION | | 62 |

## LIST OF FIGURES


| Figure | | Page |
|---|---|---|
| 1.1 | Various Soil or Soil-Tube Configurations | 2 |
| 2.1.a | Correlation of Höeg's Deformation Data Preliminary test series | 14 |
| 2.1.b | Correlation of Höeg's Deformation Data Main test series | 15 |
| 2.2 | Correlation of Donnellan's Deformation Data | 16 |
| 2.3 | Correlation of Marino's Deformation Data | 17 |
| 2.4 | Correlation of Robinson's Deformation Data | 18 |
| 2.5 | Correlation Between E* and M for Dense Sand | 24 |
| 3.1 | Theory for Buckling of Elastically Supported Ring | 29 |
| 3.2 | Coefficient of Elastic Soil Reaction for Elastic Ring | 31 |
| 3.3 | Buckling Strengths of Soil-Surrounded Tubes Upper limit | 32 |
| 3.4 | Inelastic Buckling Curves | 36 |
| 3.5 | Correlation of M.I.T. Tube Buckling Data for Shallow Depth | 44 |
| 3.6 | Limiting Values of Constrained Modulus M | 50 |
| 3.7 | Effect of Pore Pressure on Buckling Resistance | 53 |

## LIST OF TABLES


| Table | | Page |
|---|---|---|
| 2.1 | Laboratory Data on Arching Around Buried Cylinders | 8 |
| 2.2 | Backcalculated E*-values from Laboratory Tests | 13 |
| 3.1 | Intersection of Elastic Buckling Curve with Yield Stress Line for Various Materials and Soil Stiffnesses | 34 |
| 3.2 | Correlation of Donnellan's Destructive Tests | 45 |
| 3.3 | Buckling Resistance of Corrugated Cylinders | 47 |

## LIST OF SYMBOLS

| | |
|---|---|
| $A$ | a coefficient |
| $B$ | dimensionless buckling coefficient |
| $c$ | stress-strain coefficient |
| $D$ | cylinder diameter |
| $D/t_{cr}$ | critical diameter-to-thickness ratio |
| $D_h$ | horizontal cylinder diameter |
| $d$ | depth of burial |
| $E'$ | modulus of passive soil resistance (units: psi) |
| $E^*$ | modified modulus of passive soil resistance (units: psi) |
| $E_s$ | Young's modulus of soil |
| $E_t$ | tangent modulus of cylinder material |
| $EI$ | flexural rigidity of cylinder wall |
| $e$ | modulus of passive resistance (units: psi/in.) |
| $K_o$ | coefficient of lateral pressure at rest |
| $K_s$ | coefficient of elastic soil reaction |
| $M$ | constrained modulus of soil |
| $m$ | value of M-function for $\bar{p}$ = 1 psi |
| $N$ | hoop resultant normal stress |
| $n$ | buckling mode |
| $p$ | vertical soil pressure acting on cylinder |
| $\bar{p}$ | effective pressure at buckling in presence of pore pressure |
| $p^*$ | elastic cylinder buckling pressure in circular-symmetric situation |
| $p^*_{cr}$ | critical buckling pressure at $D/t_{cr}$ |
| $p_o$ | pressure applied at soil surface |
| $p^*_o$ | surface pressure causing elastic buckling |
| $p^*_e$ | surface pressure causing elastic buckling of deformed cylinder |
| $R$ | cylinder radius |
| $r_i$ | inside radius of elastic thick ring |
| $r_o$ | outside radius of elastic thick ring |

| | |
|---|---|
| $t$ | thickness of cylinder wall |
| $u$ | pore pressure |
| $\beta$ | arching factor |
| $\gamma$ | unit weight of soil |
| $\varepsilon_h$ | horizontal "strain" of cylinder |
| $\sigma_{av}$ | average stress acting on cylinder |
| $\sigma_h$ | horizontal free-field stress in soil |
| $\sigma_p$ | passive pressure on side of cylinder |
| $\sigma_v$ | vertical free-field stress in soil |
| $\sigma^*$ | elastic buckling stress ( = p* R/t) |
| $\sigma_{cr}$ | critical inelastic buckling stress |
| $\sigma_y$ | yield stress |
| $\nu$ | Poisson's ratio of soil |

BLANK PAGE

# CHAPTER 1
# INTRODUCTION

The behavior of underground flexible cylinders is of interest to both the designer of underground pipelines or culverts and the designer of protective structures. A considerable amount of research on the topic has been done by both groups of users. While originally the interests of the two groups went in different directions, a rapprochement has recently taken place, in the sense that the two groups have learned to interact with and profit from each other. An outward example of this new cooperation was the Symposium on Soil-Structure Interaction held at the University of Arizona in June 1964, where representatives from both groups came together to discuss common problems.

There is much evidence of this new-found cooperation in the recent literature. For instance, workers in protective construction have begun to appreciate more and more the classical work done on buried pipes and arching by Marston, Spangler and Terzaghi. On the other hand, workers with conventional pipe installations, faced with ever-increasing loads from high embankments for highways and dams or from heavy live loads such as airplanes, have come to realize that they derive benefits from the work on high-resistance installations done by workers concerned with protective construction.

The work done at the Massachusetts Institute of Technology over the past six years has been an attempt to introduce conventional soil mechanics knowledge and procedures into the study of the behavior of structures used in protective construction. This report represents a continuation, and in many ways a conclusion, of the work on soil-surrounded flexible cylindrical structures. The philosophy of the approach taken was to start with simple situations with respect to geometry and load application and obtain a thorough understanding of these before progressing to more complicated situations. Consequently the work progressed from hollow, thick-walled cylinders of soil (Fig. 1.1a) to circular-symmetric soil-tube

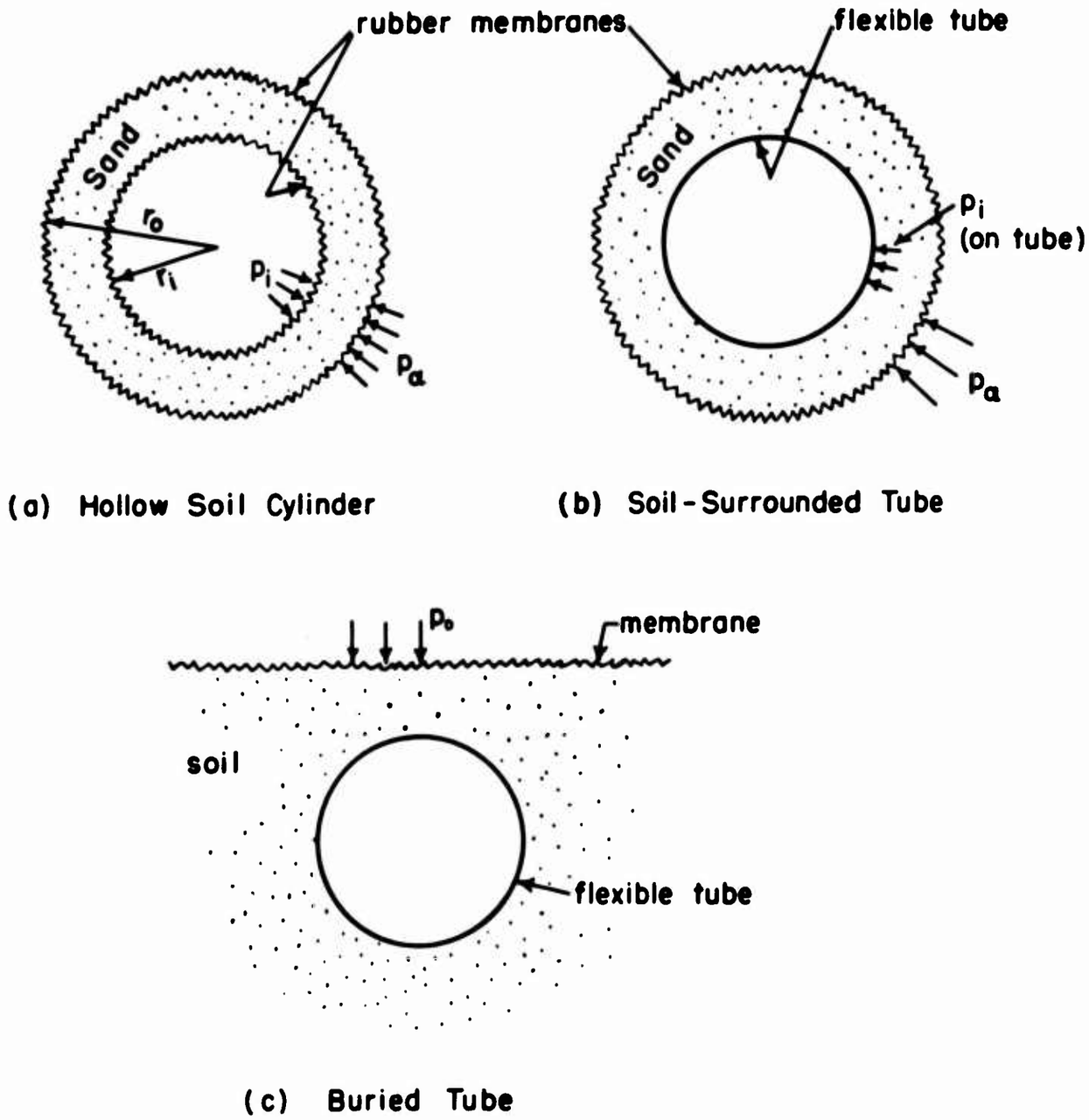


FIG. 1.1 VARIOUS SOIL OR SOIL-TUBE CONFIGURATIONS

configurations (Fig. 1.1b) to tubes buried horizontally below a soil surface (Fig. 1.1c). Consideration of dynamic loading instead of the static loading used heretofore would be a last step. This step is, however, not being planned at present, chiefly because the large-scale effort required seems more suitable for a research organization than for a university.

The last report on the progress of the research (Luscher and Höeg, 1964a) was concerned primarily with the "elastic" behavior and the collapse condition of a flexible structural tube symmetrically surrounded by soil (Fig. 1.1b). Some preliminary results from tests on flexible buried cylinders were also presented.

The present report is concerned with the behavior of flexible tubes mainly in the "buried" condition and presents an overall picture of certain aspects of cylinder behavior - arching, deformation, and buckling. The material is based on the experimental and theoretical work presented in the 1964 report mentioned above, plus pertinent information from the literature. This report thus contains no new experimental data, but rather attempts to arrive at a unified picture of the chosen aspects of behavior on the basis of a synthesizing study of existing data and theories.

A companion report prepared by K. Höeg (1965) describes a new study of the interaction between underground structural cylinders and the surrounding soil. A mathematical formulation considers soil to behave as a continuous, elastic material. The applicability of the analytical approach was tested in the experimental phase of the study, with experiments designed to measure directly the contact pressures between sand and buried cylinders. The variables were cylinder flexibility, cylinder compressibility, depth of sand cover and level of applied surface pressure.

The condition specifically investigated in the present report is that of a long, flexible, cylindrical tube buried in horizontal position below a horizontal soil surface and loaded by static pressures applied on that surface (Fig. 1.1c). If the depth of burial is at least "full," corresponding to a depth of cover of one to two tube diameters, this case

is no different from the case of a tube loaded by a high earth fill.

Chapter 2 is concerned with a number of aspects of the behavior of buried flexible cylinders - arching, deformation, failure condition. The information was gathered as much for its own sake as to provide inputs for the subsequent chapter, Chapter 3, which treats buckling of buried flexible cylinders. This work on buckling represents an extension and conclusion of the earlier research by the author (Luscher and Höeg, 1964a). It extends the theory for buckling of soil-supported tubes from the circular-symmetric situation to the buried-tube situation, into the inelastic range, to buckling of corrugated pipes, and to more general conditions of soil surrounding. General conclusions are reached about the importance of buckling as a possible failure mode for flexible buried cylinders.

# CHAPTER 2

# BASIC CONCEPTS OF BEHAVIOR OF FLEXIBLE CYLINDERS

## 2.1 INTRODUCTION

This chapter quantitatively evaluates certain aspects of the response of buried cylinders. The information was gathered from numerous recent publications concerned with cylinder behavior. The purpose is to set the stage for the subsequent chapter on buckling, by relating buckling failure to the other possible modes of failure and by providing needed numerical inputs on arching and tube deformation. Thus this chapter is not meant to cover all aspects of the behavior of flexible cylinders, but rather to present information of general interest collected in connection with the investigation of buckling.

The free-field stresses in a dry soil mass are a vertical stress $\sigma_v = \gamma h + p_o$ and a horizontal stress $\sigma_h = K_o \sigma_v$, where $\gamma h$ is the weight of the soil surcharge, $p_o$ is the uniform pressure applied at the soil surface (over a large area), and $K_o$ is the coefficient of lateral pressure at rest. In general $K_o$ might vary from 0.35 to 0.7 for most soils except heavily overconsolidated clays. If an inclusion, in the present case a buried cylinder, deformed just like the soil, it would be exposed to these stresses. However, a flexible cylinder has only a limited capacity to withstand these highly uneven stresses and will start to deform into a shape resembling a horizontal ellipse. In so doing it mobilizes lateral passive soil stresses which counteract the deformation. Under increasing applied loads the cylinder will further deform in such a way as to carry the load most efficiently; it will be exposed to large hoop compression stresses, but the bending moments will be small compared to the bending moments which would be required to carry the free-field stress system with no soil support. Eventually the cylinder will fail in one of several possible failure modes.

The important questions associated with loading of the cylinder-soil

system are:

1. How is the hoop stress related to the free-field stresses, i.e., what is the arching condition?

2. What is the deformation of the pipe?

3. What is the condition of failure?

The following sections will discuss these three questions in turn.

## 2.2 ARCHING

How much stress, in relation to the free-field stress system, reaches the buried cylinder? It is clear in this context that not the extremely low flexural rigidity of an unsupported cylinder, but rather the much higher vertical rigidity of the soil-supported cyliner, or possibly even the compressive (volumetric) rigidity, should be compared to the rigidity of the soil when investigating arching.

Arching was studied by Luscher and Höeg (1964a) in connection with tests on circular-symmetric tube-soil configurations (Fig. 1.1b). It was found for the particular situation investigated that the stress carried by thin-walled aluminum tubes was within ± 20 percent of the stress applied on the outside of the soil cylinder, with individual values depending on soil density and soil-ring thickness. Thus, only little arching action took place. The experimental result agreed with the developed elastic theory, which indicated that the compressibility of the tube in the pure compression mode (mode zero) was similar to the compressiblity of the surrounding sand ring. In tests using plastic tubes with much higher compressiblity, on the other hand, very effective active arching was mobilized in the sand ring; the share of the applied stress carried by the tube dropped to as little as 20 percent.

For tubes in a buried configuration (Fig. 1.1c), one might expect the horizontal ellipsing, which is associated with vertical shortening, to lead to a reduction in vertical applied stress on account of arching.

If without deformation the vertical stress is $\sigma_v$ and the horizontal stress $K_o\sigma_v$, then the more-or-less uniform stress $\sigma_{av}$ after deformation might be expected to be the average of the two, or $\frac{1}{2}(1 + K_o)\sigma_v$. This type of arching, which was called "pressure redistribution" by Luscher and Höeg (1964b), thus derives from the increase in vertical compressibility due to ellipsing of the tube. Since the ellipsing is the principal effect which distinguishes the buried-tube case from the circular-symmetric case, no further appreciable arching effects (beyond pressure redistribution) would be expected for flexible metallic tubes, where the compressibility of the tube in the zero mode is roughly comparable to the compressiblity of the surrounding soil.

Evidence exists that the above concepts are correct, at least for dense sand. Preliminary test data reported by Luscher and Höeg (1964a) indicated that the applied surface pressure at buckling of a tube in a rigid box loaded only at the surface ($K_o$ stress system) was 50 percent higher than the surface pressure of a tube in a box loaded equally in vertical and horizontal direction. (If $K_o = 0.4$, $\frac{1}{2}(1 + K_o) = 0.7$. Thus a tube in the first situation "feels" only 70 percent of the surface pressure, while a tube in the second situation "feels" 100 percent. If the stress leading to tube failure is the same in both cases the surface pressures at failure can therefore be expected to be in the proportion 10 to 7, which is close to the observed $1\frac{1}{2}$ to 1.).

A considerable body of evidence from tests on flexible, metallic tubes of 4- to 6-in. diameter, buried at a depth of one-half to two tube diameters in dense sand is summarized in Table 2.1 (Luscher, 1965; Donnellan, 1964; Marino, 1963; Robinson, 1962). The tubes were strain-gaged inside and out, making it possible to determine hoop stress resultants. The value of the measured hoop force on the sides, indicative of the total vertical load carried by the tube, varied between 33 and 100 percent of applied load, with an average just under 70 percent. The average of the hoop forces at top and bottom, indicative of the total horizontal load carried by the tube, was somewhat lower than the force on the sides and averaged 50 percent of applied loads. The depth of cover within the quoted limits had very little effect upon these values, as shown clearly by Donnellan's (1964) data. The variation in D/t over the range 80 to 120

TABLE 2.1 LABORATORY DATA ON ARCHING AROUND BURIED CYLINDERS

| Reference | Soil Type | Tube Type | Depth of Cover | Pressure range psi | Percentage of applied load carried by tube | Remarks |
|---|---|---|---|---|---|---|
| Luscher (1965) | dense Ottawa sand | aluminum D = 4 in. D/t = 114 | ½D | 0-100 | sides 50<br>top 20-30<br>bottom 100-85 | |
| | loose Ottawa sand | aluminum D = 4 in. D/t = 114 | ½D | 0-50 | sides 130-150<br>top 30-40<br>bottom 60-80 | |
| Donnellan (1964) | dense Ottawa sand | aluminum D = 4 in. D/t = 114 | ½D-2D | 0-140 | sides 33-50<br>top 25-40<br>bottom 25-45 | most extensive test series; extremely dense sand |
| | | aluminum D = 4 in. D/t = 250 | ½D-2D | 0-50<br>0-140 | sides 15-60<br>top 0-35<br>bottom 12-25 | inconsistent data |
| Marino (1963) | dense Ottawa sand | steel D = 5 in. D/t = 80 | 2D | 0-400 | sides 85<br>top 75<br>bottom 45-50 | soil density probably not as high as in Luscher's and Donnellan's tests |
| Robinson (1962) | dense Ottawa sand | steel D = 6 in. D/t = 120 | 2½D | 0-100 | sides 80-90<br>top 70-75<br>bottom 50-70 | soil density probably not as high as in Luscher' and Donnellan's tests |
| | | steel D = 6 in. D/t = 80 | 2½D | 0-100 | sides 85-95<br>top 45-50<br>bottom 40 | |
| | | aluminum D = 6 in. D/t = 120 | 2½D | 0-100 | sides 75-80<br>top 40-45<br>bottom 33-50 | |

and the tube material also had only small effects (Robinson, 1962). The major variable seems to have been a personal one, evidenced probably mainly in the soil density, but also in the method of placement of the tube, test device used, instrumentation etc. The only known data of this kind for loose sand (Luscher, 1965), also presented in Table 2.1, indicated side hoop forces up to 50 percent higher than the applied load, and averaged top and bottom hoop forces 40 to 60 percent of applied load. Höeg (1965) presents data from tests with direct measurement of contact stresses which show that the average stress applied on a steel tube with D/t = 80 buried at 1D depth in dense Ottawa sand was about 70% of the applied surface pressure.

It can be concluded that for flexible, metallic tubes buried in dense sand, the hoop forces are somewhat smaller than the vertical applied load on account of pressure redistribution and arching. This reduction has been observed to be anywhere between 0 and 70 percent, with an average of about 30%. For loose sand, the little available evidence indicates no such beneficial action, rather the possibility of some increase in pressure acting on the tube due to passive arching. These statements can be summarized in the highly approximate equation

$$p = p_o/\beta \tag{2.1}$$

where $\beta$ = 1.5 for stiff soil and 1.0 for compressible soil.

The above concepts of loads acting on underground cylinders are extremely crude. Their only merits are that they are simple, and that they originate from - however limited - experimental evidence. Marston's and Spangler's work (Spangler, 1960) resulted in a complete system of recommendations for loads on buried conduits. However, these theories were derived and verified primarily for rigid pipes and are therefore unacceptable here in connection with flexible cylinders. More recently, several arching theories have been developed based mainly on the concept of vertical slip surfaces (e.g., Newmark and Haltiwanger, 1962; Finn, 1963; Allgood, 1965). Use of any of these theories would require additional

numerical inputs, the end result could not be expressed in the simple form of Eq. (2.1), and it is not even certain that the result would be any more trustworthy.

## 2.3 DEFORMATION OF FLEXIBLE CYLINDERS

### 2.3.1 Deformation Equation

The standard method to predict deformations of buried cylinders is by way of Spangler's (1960) equation, which may be written as

$$\varepsilon_h = \frac{\Delta D_h}{D} = \frac{p}{85\ EI/D^3 + 0.65\ E'} \quad , \qquad (2.2)$$

where $\varepsilon_h$ = horizontal "strain"
$\Delta D_h$ = change in horizontal diameter
$D$ = cylinder diameter
$EI$ = flexural rigidity of cylinder wall
$p$ = vertical soil pressure acting on cylinder
$E'$ = modulus of passive resistance of soil.

The coefficients in the denominator were calculated for a deflection lag factor of 1.0 and a bedding constant of 0.094, corresponding to a bedding angle of $50^o$.

This equation appears to be basically sound. However, there are a number of difficulties associated with its use. One of the difficulties is the choice of a value for the applied pressure p, which is usually calculated by the Marston-Spangler theories of loads on underground conduits (Spangler, 1960) and involves a number of critical assumptions. Further, in the derivation of the equation the fact was neglected that even without any deformation the lateral pressure would not be zero, but $K_c\ \sigma_v$. Thus, considering also pressure redistribution as discussed in the preceding section, the vertical pressure which has to be resisted by the combination of the tube rigidity and lateral passive pressure

is not $\sigma_v$, but rather (for dense soil)

$$\sigma_{av} - K_o \sigma_v = \tfrac{1}{2}(1 + K_o)\,\sigma_v - K_o \sigma_v = \tfrac{1}{2}(1 - K_o)\,\sigma_v.$$

The primary difficulty with the use of Eq. (2.2) is associated with the choice of E'. Recommendations for this choice have been formulated (ASCE, 1964). However, such "handbook" values can only be crude estimates since crude soil identification is used rather than tests on the actual soil, and consequently a high factor of safety is required. Furthermore, these recommendations are for constant E'-values, and thus cannot predict the curved load-deformation relationship frequently observed.

To improve on this situation, an attempt was made to correlate tube deformations measured in several recent tests and test series with the theory, i.e., to backcalculate E'-values from experimental data. First Eq. (2.2) had to be modified according to the ideas presented above. The following assumptions were made for this modification:

1. To account for pressure redistribution and arching as well as at-rest lateral pressure, p in the equation is set equal to $1/3\,\sigma_v$ (which is about equal to $\tfrac{1}{2}(1 - K_o)\,\sigma_v$) for dense soil, and $\tfrac{1}{2}\,\sigma_v$ for loose soil.
2. If E' is variable with pressure, the equation is applied incrementally, relating $\Delta\varepsilon_h$ to $\Delta\sigma_v$; the total horizontal strain $\varepsilon_h$ is then the sum of all increments up to the pressure under consideration.

With these assumptions, the deformation equation becomes

$$\Delta\varepsilon_h = \frac{0.5/\beta \cdot \Delta\sigma_v}{85\,EI/D^3 + 0.65E^*} \qquad (2.3)$$

where $\beta$ = 1.5 for dense soil ($0.5/\beta = 1/3$)
1.0 for loose soil ($0.5/\beta = 1/2$)

$E^*$ = $f(\sigma_v)$ is a modified modulus of passive resistance of soil (defined differently because of the modification in the load term).

The form of the E*-function will in general be assumed as a power function, $E^* = C\,\sigma_v^{\,b}$. If the tube rigidity term 85 $EI/D^3$ is negligible compared to the soil term 0.65E*, the expression for $\Delta\varepsilon_h$ can be integrated to give a direct solution for $\varepsilon_h$ as a function of $\sigma_v$. On the other hand, if the tube rigidity is considered and E* is a function of $\sigma_v$, a numerical, step-by-step solution is best used.

### 2.3.2 Experimental Evidence

Recent tube deformation data from various sources were used to determine, by substitution into Eq. (2.3), the function $E^* = C\,\sigma_v^{\,b}$ which best satisfied the experimental load-deformation curves. In some cases where only final deformations but no load-deformation curves were available, only constant values of E* could be determined. In two cases where the load-deformation curve was a straight line over the region of interest, a constant value of E* was also calculated. In all other cases locking behavior was apparent, i.e., the rate of tube deformation decreased with increasing applied pressure. While every curve could be fitted with one best E*-function, with an exponent b which might lie anywhere between zero and one depending on the character of the curve, it became soon apparent that a square-root function

$$E^* = C\,\sigma_v^{\frac{1}{2}}$$

gave the best fit overall. Thus each of the available load-deformation curves was fitted with a theoretical curve based on an E*-function of this type.

The results of fitting several quite similar laboratory experiments, all involving tubes of 4- to 6-inch diameter buried at a depth of at least D in dense sand, are presented in Table 2.2 and Figs. 2.1 through 2.4 (Höeg, 1965; Donnellan, 1964; Marino, 1963; Robinson, 1962). The table and figures show that all four series of tests gave amazingly consistent E*-values of between 1900 $p_o^{\frac{1}{2}}$ and 3000 $p_o^{\frac{1}{2}}$, with an average of about 2400 $p_o^{\frac{1}{2}}$. The one-half power law gave on the average the best fit, as it resulted in load-deformation curves which were "best-fit" in some cases, too much curved in

TABLE 2.2 BACKCALCULATED E*-VALUES FROM LABORATORY TESTS

| Reference | Soil Type | Tube Type | Pressure Range-psi | E* psi | Comments on Fit | General Comments |
|---|---|---|---|---|---|---|
| Höeg (1965) | dense Ottawa sand | steel, D=4½ in. D/t=28, 46, 68 | 0-150 | $2400\ p_o^{\frac{1}{2}}$ | good for D/t=46,68 not good for D/t=28 | negative arching at low pressures must be responsible for bad correlations for rigid tubes. |
| | | steel, D=4½ in. D/t=40, 80 | 0-150 | $1900\ p_o^{\frac{1}{2}}$ | good for D/t=80 not good for D/t=40 | |
| Donnellan (1964) | dense Ottawa sand | aluminum 6061-T4, D=4 in., D/t = 114 | 0-140 | $3000\ p_o^{\frac{1}{2}}$ | good | extremely dense sand. Because of high arching, used $\beta = 2.0$ |
| Marino (1963) | dense Ottawa sand | steel, D=5 in. D/t = 80 | 0-400 | $2200\ p_o^{\frac{1}{2}}$ | reasonable | a 2/3-power law would give excellent fit |
| Robinson (1962) | dense Ottawa sand | steel, D=6 in. D/t = 80, 120 | 0-100 | $2500\ p_o^{\frac{1}{2}}$ | good | a lower power of p would give better fit |
| | | aluminum, D=6in. D/t = 120 | 0-100 | $2700\ p_o^{\frac{1}{2}}$ | reasonable | unreliable deformation data (due to local deformations) |

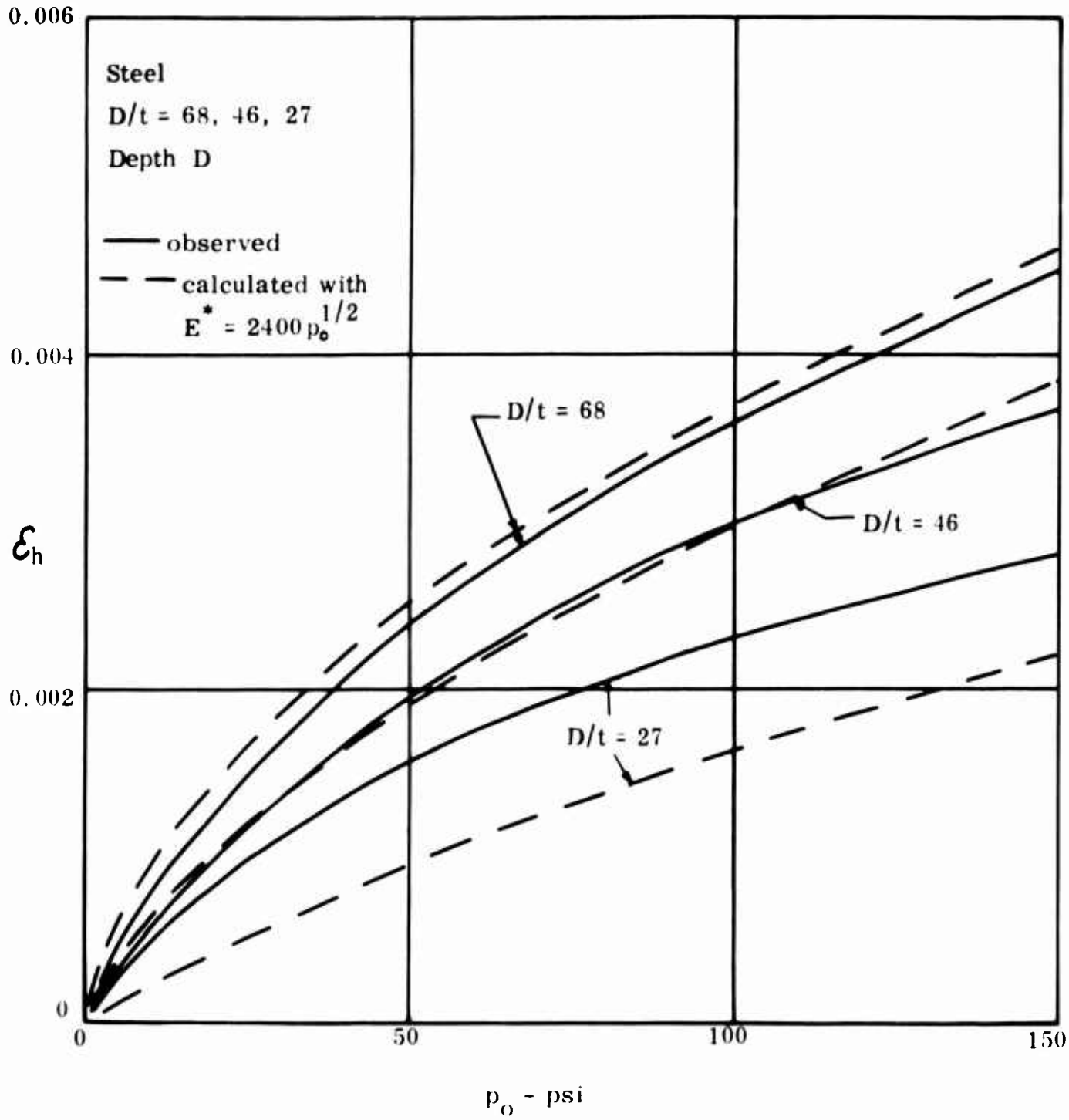


FIG. 2.1.a CORRELATION OF HÖEG'S DEFORMATION DATA
Preliminary Test Series

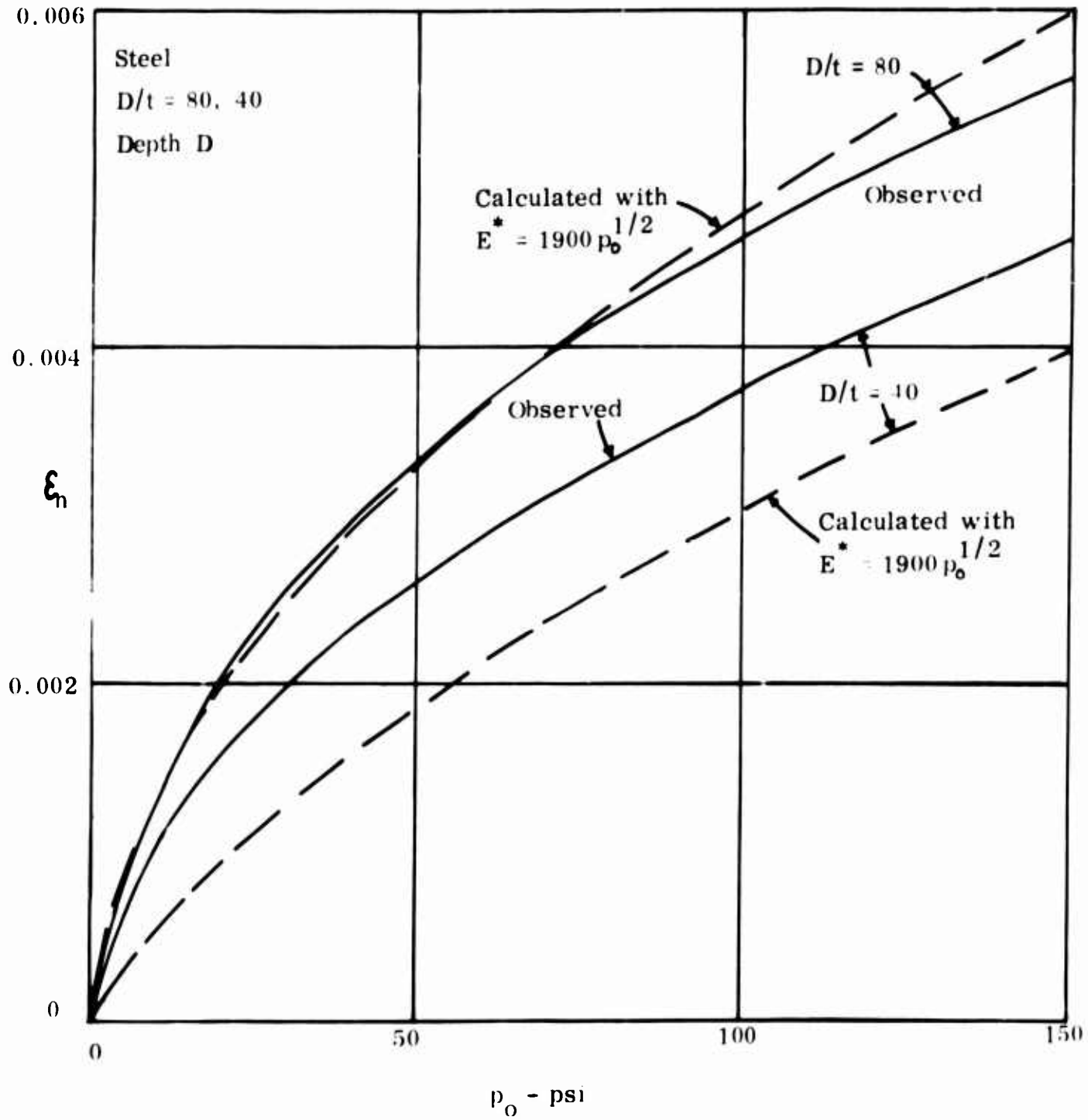


FIG. 2.1.b CORRELATION OF HÖEG'S DEFORMATION DATA
Main Test Series

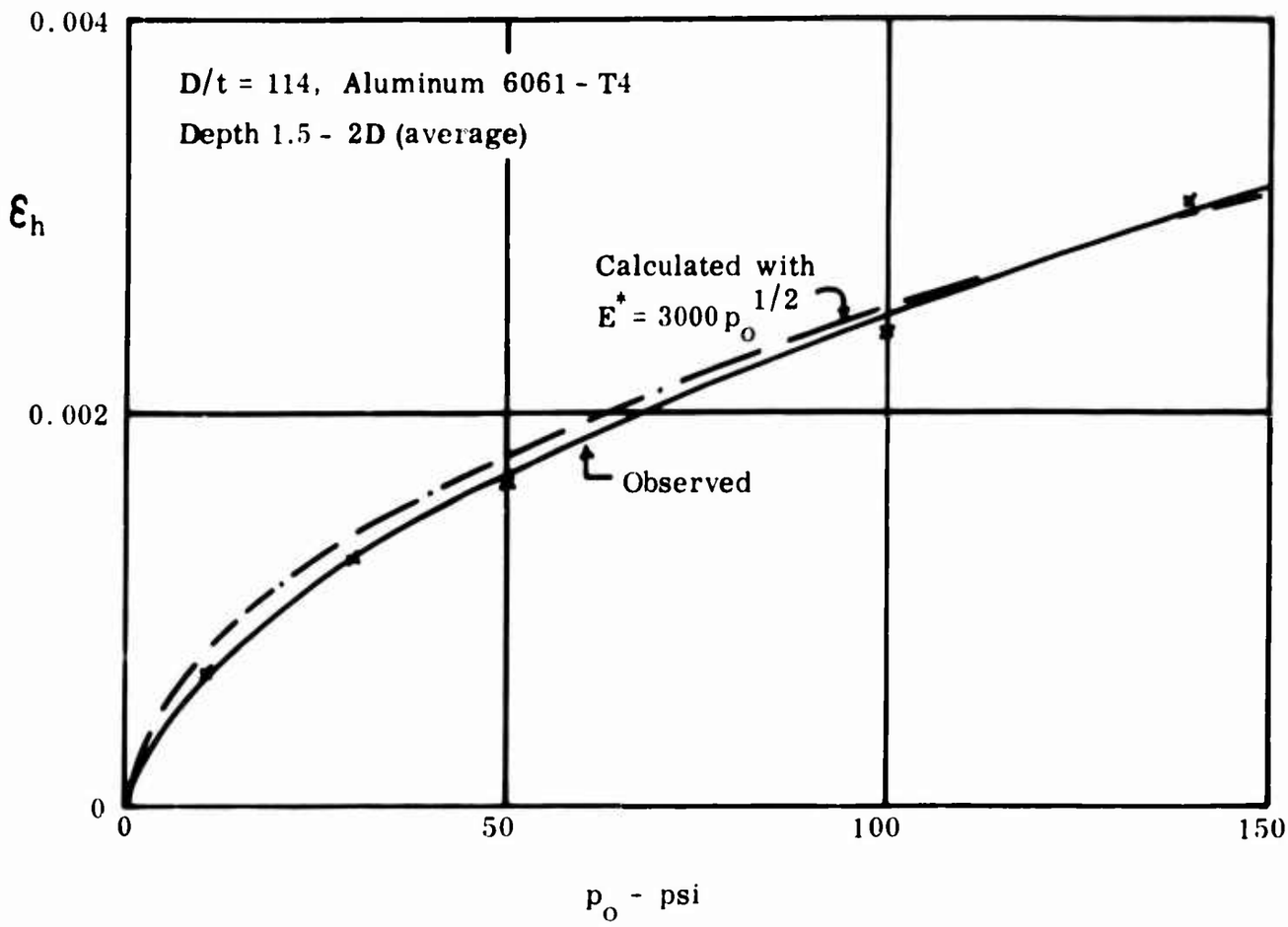


FIG. 2.2 CORRELATION OF DONNELLAN'S DEFORMATION DATA

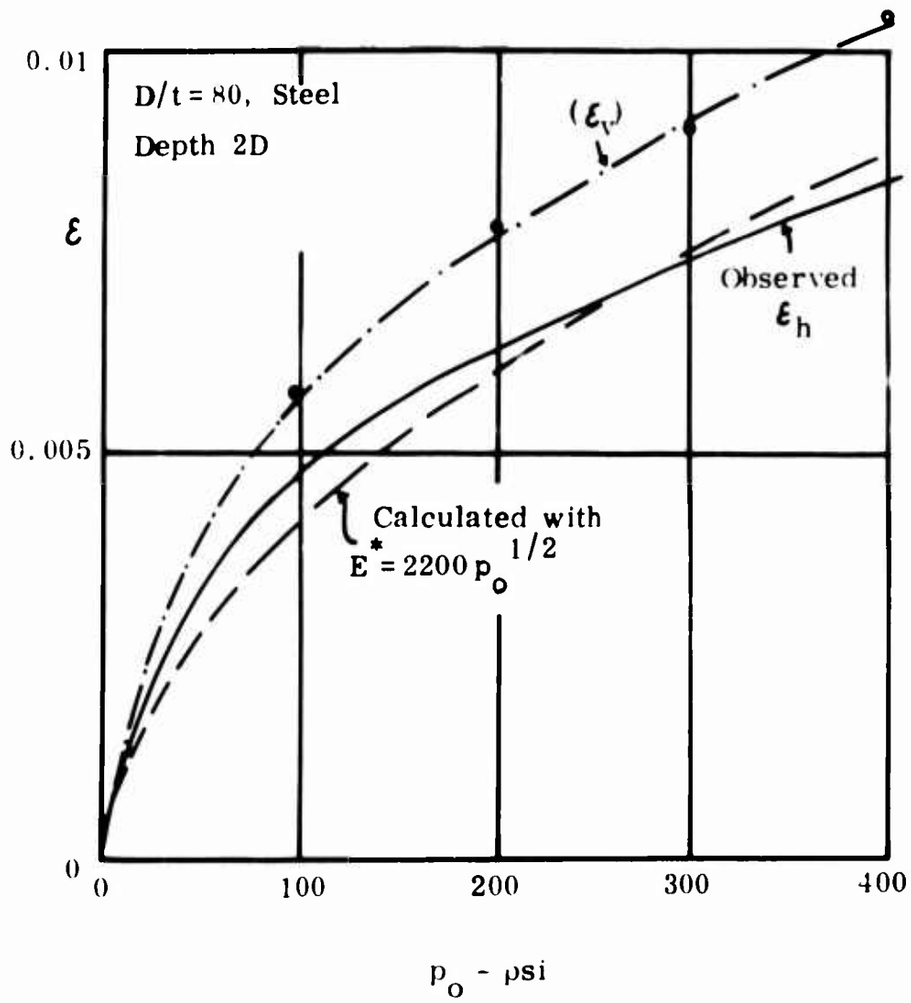


FIG. 2.3 CORRELATION OF MARINO'S DEFORMATION DATA

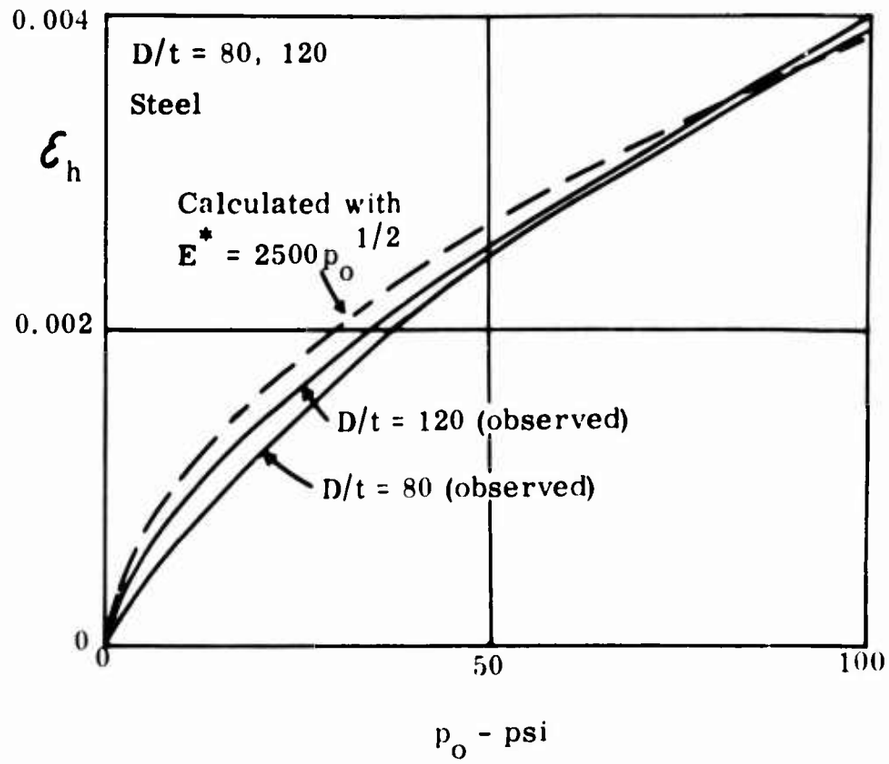


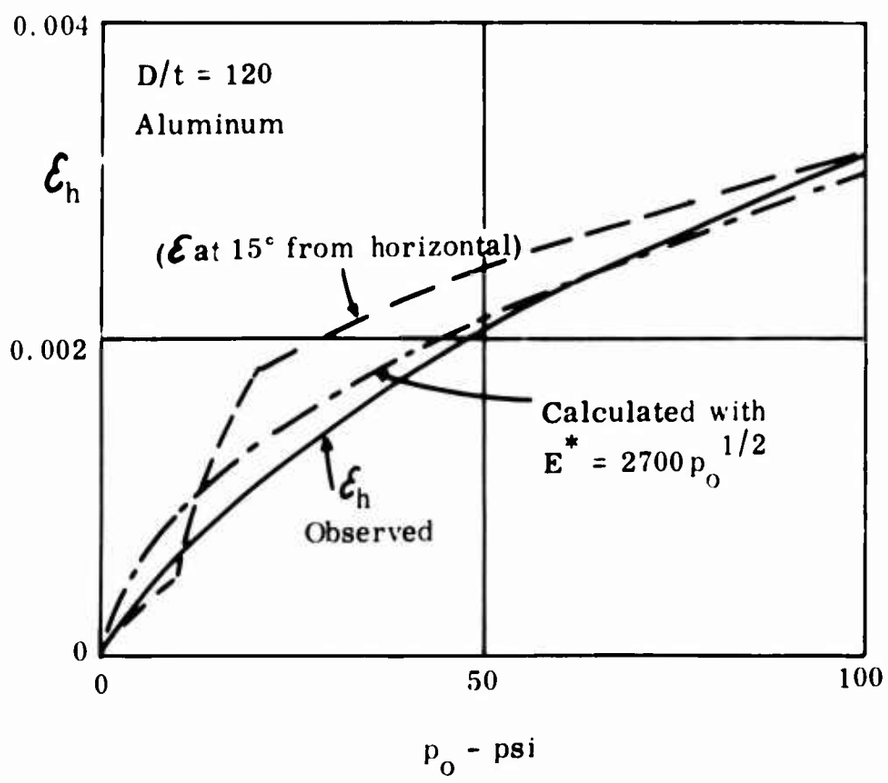


FIG. 2.4 CORRELATION OF ROBINSON'S DEFORMATION DATA

others and not enough curved in still others. Thus, one can summarize by saying that a value of at least

$$E^* = 2000\,\sigma_v^{\frac{1}{2}} \tag{2.4}$$

was reached quite consistently in laboratory tests using carefully placed, dense sand.

Allgood (1965) presents data on a steel tube of 24-in. diameter and D/t = 500 buried at 3/8 D depth in "dense" Monterey sand. The straight load-deformation curve in the pressure range 12 - 25 psi (well beyond a previously applied pressure of 10 psi) resulted in an E*-value of 3800 psi. Over the same range of pressures the experiments summarized in Table 2.2 gave E*-values between 7500 and 12,000 psi. Allgood's smaller value must be due to the smaller depth of cover and probably a smaller relative density of the sand; the latter possiblity is quite high in view of the large soil volume that has to be placed in the test pit of the NCEL atomic blast simulator.

An example of the effect of backfill density in laboratory studies is given by Luscher's (1965) data from dynamic tests on buried aluminum tubes of 4-in. diameter. The results were:

dense sand (relative density 90%): $E^* = 2100\,\sigma_v^{\frac{1}{2}}$

loose sand (relative density 30%): $E^* = 950\,\sigma_v^{\frac{1}{2}}$.

Effects other than soil density may have had an influence on the relative values of the deformations in dense and loose sand (e.g. arching, or different dynamic effects). However, direct comparisons of this kind are rare enough that it was felt these data should be included here. Furthermore, the excellent agreement of the E*-values for dense sand with the data in Table 2.2 indicates that for this situation the dynamic character of the loading did not alter the deformations appreciably. It can reasonably be assumed that the data for loose sand are just as representative for that density.

Bulson (1962) presents deformation data for very flexible steel tubes with D = 10 in. and D/t = 667, buried at a depth of 3/4 D in

"compacted sand" which was probably of medium to low density. The resulting E* was almost constant at 1100 psi with pressure up to 40 psi. There are, however, uncertainties associated with rigid-body motion, with the ratio of horizontal to vertical deformation, and with the relative density of the sand which make this value highly tentative.

The remaining correlations are for field case studies. Since in all these cases no load-deformation curves but only final deformations were available, constant values of E* were backcalculated.

E*-values for field installations of pipes of 30-in. diameter and 0.312-in. wall thickness can be obtained from Lambe (1960, 1963). For two different pipes installed without any control of the granular backfill, the values were 1100 and 750 psi. For pipes carefully backfilled to minimize deformations and loaded by a fill of 75-ft. height, on the other hand, E* was backcalculated to be at least 7000 psi.

Barnard (1957) quotes some data on two instrumented pipe situations. The first of these, a smooth pipe with 30-in. diameter and 0.109-in. wall thickness, showed a horizontal diameter change of 0.32 in. under 12 ft. of "tamped-sand" fill. The resulting E* for this probably quite loose fill was 600 psi. The second case, a 1-gage multi-plate pipe of 7-ft. diameter under 137 ft. of fill, yielded E* = 2700 psi for a carefully placed backfill. These two E*-values are probably quite typical of the possible range in field installations.

When comparing these backcalculated values of E* with published values of E', it should be borne in mind that the E*-values were obtained from Eq. (2.3) and therefore are reduced by a factor of 2 to 3 compared to E' on account of the initial assumptions made (arching, lateral at-rest pressure). Thus E*-values should be multiplied by a factor 2 to 3 when they are compared to published or generally accepted values of E'; inversely, published values of E' should be reduced by that factor when they are to be used as E* in Eq. (2.3).

These comments apply to Watkins's (1959) work, which led to E'-values (calculated by Eq. (2.2)) of 1500 to 4000 psi for laboratory tests on mixtures

of silt and clay of varible known density, but unknown water contents. On the other hand, values obtained in the so-called Modpares device are direct measurements of the modified passive soil modulus E* and should therefore be directly comparable to the values backcalculated here. ASCE (1964) contains such values, which are "suggested as a guide" (quoting from publication) and contain a built-in safety factor of as much as 2. The values vary between 720 and 4400 psi for sand at various densities, and between 540 and 4020 for clay at various densities.

The information on values of E* backcalculated from test results and quoted in the literature may be summarized as follows:

1. For granular soil, carefully placed under laboratory conditions to achieve maximum density, the load-deformation curve exhibits locking character. This is expressed by an E* which increases with a positive power of the applied pressure. The conservative relationship

$$E^* = 2000\,\sigma_v^{\frac{1}{2}} \quad (E^* \text{ and } \sigma_v \text{ in psi}) \qquad (2.4)$$

   describes well the results of several recent test programs. It corresponds to average values of about 3000, 7000 and 14,000 psi for the pressure ranges 0-10, 0-50 and 0-200 psi, respectively.

2. Very little evidence exists for laboratory E*-values of loose granular soil and cohesive soil of any consistency. Values ranging from 700 to 3000 psi for loose sand, and from 500 to 6000 psi for cohesive soil are mentioned in the literature.

3. In field installations with well-controlled backfill, E*-values of 3000 psi or higher have been achieved.

4. For field installations with very little or no backfill control, values of E* in granular soil appear to be at least 500 psi. No corresponding minimum value could be established for cohesive soil.

It should be pointed out again that all values quoted above are for use with Eq. (2.3). For use with Eq. (2.2) the E*-values should be increased by a factor 2 to 3. Eq. (2.3) is believed to be preferable to Eq. (2.2) since it considers arching and lateral at-rest pressures.

### 2.3.3 Correlation of E* with Compression Test

The remaining question is: Can the E*-values quoted in the preceding section be correlated to any soil property obtainable in a standard soil test? The locking behavior observed in many cases indicates that the correlation should be made to the one-dimensional compression test rather than the triaxial test. Therefore, the laboratory data for granular soils will be compared with data from one-dimensional compression tests on Ottawa sand, taken from Fig. 4.3 of Luscher and Höeg (1964a) and reproduced as Fig. 2.5 of this report.

To undertake this correlation between E* and the constrained modulus M, a theoretical relationship must be established between the two moduli. E* can be expressed as

$$E^* = eR,$$

where e is the modulus of passive resistance, in units of psi/in. Now e can be related to M by a simple pressure-bulb consideration. The lateral passive pressure is usually assumed to act with parabolic distribution over the middle 100° on the sides of the pipe (Spangler, 1960). As equivalent "footing width," two thirds of the chord subtended by a central angle of 100° is used, or 0.51 D ( = width of uniformly loaded rectangular strip with peak pressure equal to that of a parabolically loaded strip). A reasonable depth of an equivalent pressure bulb with triangular stress distribution has been found to be 3.25 times the width of the loaded area (Barnard, 1957), or 1.67 D. Then, using $E_s$ = 0.75 M (Luscher and Höeg, 1964a) as modulus in the pressure bulb,

$$\frac{\Delta D_h}{2} = \frac{\sigma_p}{2} \frac{1.67\ D}{0.75\ M}$$

Thus, $$e = \frac{\sigma_p}{\Delta D_{h/2}} = \frac{1.5\ M}{1.67\ D},$$

which leads to $E^* = 0.45\ M.$[1)]

Accordingly, the laboratory E*-values for granular soil from the preceding section were multiplied by a factor 2.2 to obtain values of M, which were then plotted in Fig. 2.5. The curves were not plotted in the lowest pressure range because the observed load-deformation curves and consequently the backcalculated E*-values are poorly defined in that region. It was found that the relationships for both dense and loose sand agreed reasonably well with the corresponding values obtained in one-dimensional compression tests.

Thus the conclusion is reached that the modified modulus of lateral pressure E* can, at least for granular soil, be correlated with the one-dimensional modulus M:

$$E^* \approx 0.45\ M. \qquad (2.5)$$

This relationship was derived theoretically by a simple pressure-bulb consideration and agreed well with experimental data.

## 2.4 FAILURE OF FLEXIBLE CYLINDERS

The possible structural failure modes of a flexible cylinder buried

---

1) Note that this result is somewhat different from Barnard's (1957), which would be E* = 0.3 M. Barnard used the full width of the chord as "footing width", while here a factor 2/3 is added to account for the parabolic stress distribution. The same result of E* = 0.45 M would be obtained if Barnard's "footing width" were used and the applied uniform pressure reduced by a factor 2/3. Exact numbers are not important here in view of the generally approximate nature of the calculations; the important point is that these considerations indicate that E* should be roughly 2 to 3 times smaller than M.

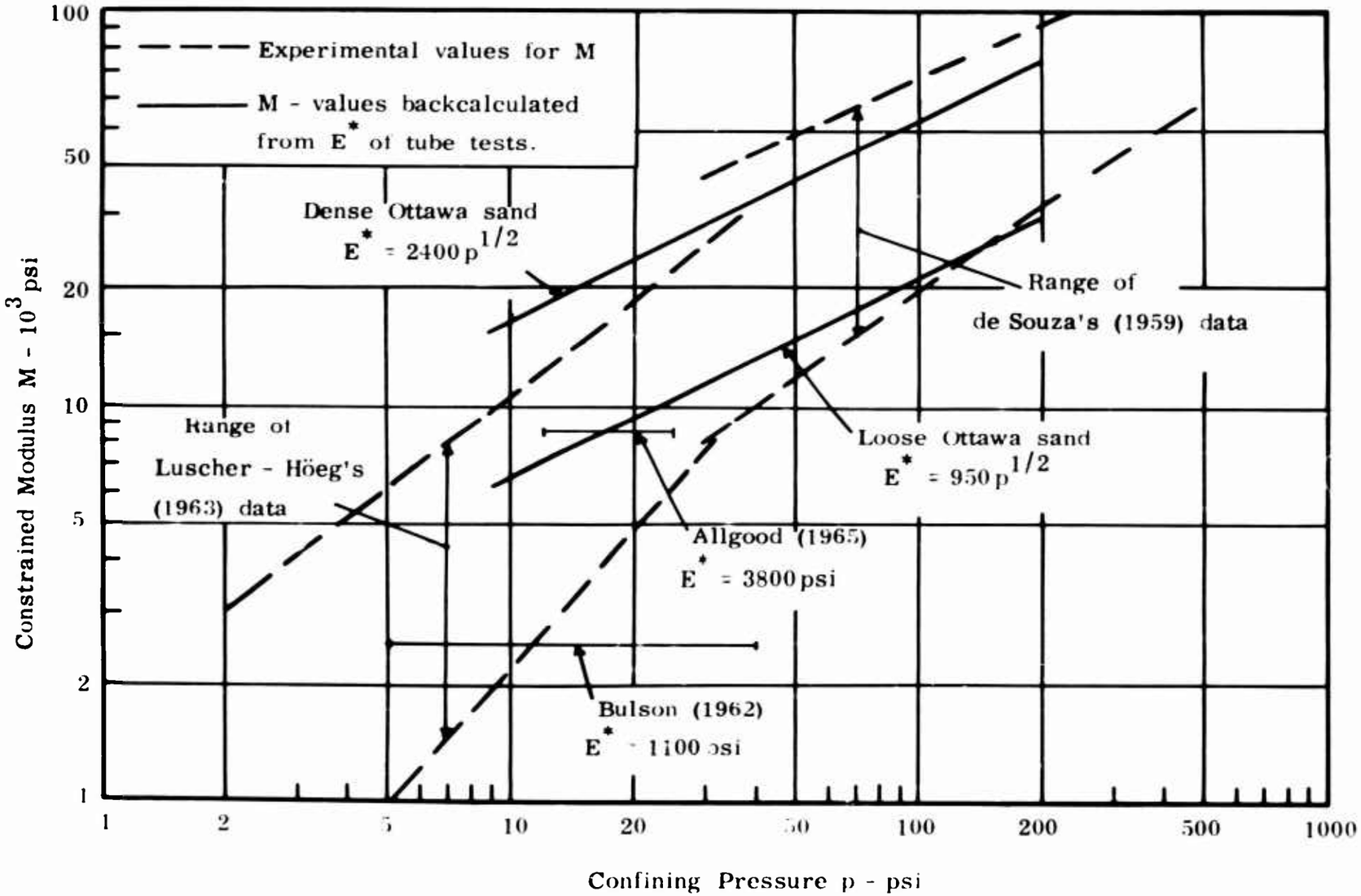


FIG. 2.5 CORRELATION BETWEEN $E^*$ AND M FOR DENSE SAND

at a depth of at least one diameter are:

1. Joint failure
2. Excessive deformation leading to caving-in of the crown of the tube.
3. Elastic buckling of the tube wall under hoop stresses which are excessive for the tube rigidity and lateral support provided.
4. Yielding of the tube wall due to excessive hoop stresses, resulting in general crushing unless such a failure is closely preceded by plastic buckling due to decrease in wall rigidity.

Of these failure modes the last one is most desirable, since it represents most efficient use of the structural materials and will, for a given situation, take place at the highest pressure. The other modes are forms of premature failure that should in general be avoided, if possible.

Failure by excessive deformation (be it defined as above, as collapse induced by excessive deformation, or as failure to function satisfactorily due to excessive deformation) can generally be avoided by appropriate control of the backfill on the sides of the cylinder. Cases where this presents difficulties, and where deformation may thus remain the controlling factor, are 1) bored tunnels, where no control over the backfill is possible, and 2) cases where the allowable deformations are small because of the function of the cylinder (e.g., carrier pipes, as discussed in Lambe, 1960). The situation with respect to deformations can frequently be improved by installing the cylinder with vertical "ellipsing," i.e., with the vertical diameter somewhat increased by fabrication or by installation of struts.

Premature joint failure can always be avoided by constructing joints to at least the full strength of the cylinder wall.

Buckling is the remaining possible mode of premature failure.

It is well known that a flexible cylinder loaded by outside liquid pressure has low buckling resistance. When the stress on the cylinder is applied through soil, however, the danger of buckling is greatly reduced on account of the shear strength of the soil. It is of great practical interest to know by how much the buckling resistance is increased. This topic is discussed in the following chapter.

CHAPTER 3

# BUCKLING OF FLEXIBLE UNDERGROUND CYLINDERS

## 3.1 INTRODUCTION

In this chapter a solution will first be presented for the most basic case of buckling of a soil-surrounded tube: that of elastic buckling of a circular tube with a surrounding thick cylinder of one specific soil and loaded by uniform radial pressures. The theory for this case has been developed quite recently and has been verified experimentally for a limited range of tube stiffnesses and soil conditions.

In subsequent sections deviations from this most basic case are investigated. These extensions of the buckling theory were derived theoretically, and were verified by existing experimental evidence wherever possible. The specific cases considered were the following: Section 3.3 discusses inelastic buckling. Sections 3.4 and 3.5 treat the effects of burial, i.e., of the change in geometry from circular-symmetric to underground with load applied at the surface; Section 3.4 is concerned with the "fully-buried" case where the effects of the soil boundary are negligible, while Section 3.5 investigates the effects of a near-by soil boundary (shallow burial). The buckling resistance of corrugated pipes is studied in Section 3.6. Finally, Section 3.7 explores the effects of soil stiffness and of the presence of pore pressure on the buckling resistance.

## 3.2 ELASTIC BUCKLING OF SOIL-SURROUNDED, SMOOTH CYLINDERS

The theory for elastic buckling of an elastically supported cylinder predicts instability under an average applied outside pressure $p^*$ of

$$p^* = 2\sqrt{\frac{K_s EI}{R^3}}, \qquad (3.1)$$

where $K_s$ = coefficient of elastic soil reaction.
For a derivation of this equation, see Link (1963), Luscher and Höeg (1964a), or Allgood (1965).[2] The relationship is plotted in Fig. 3.1 for a fixed value of the term $EI/R^3 = 1.0$, corresponding to a flexible tube ($D/t = 280$ for steel). The theory further indicates (Luscher and Höeg, 1964a) that the critical buckling mode $n$ is

$$n = \sqrt[4]{\frac{K_s R^3}{EI}} \quad . \tag{3.2}$$

The buckling modes are also indicated in Fig. 3.1 [2]

The task of predicting the critical buckling condition is thus reduced to finding the coefficient of elastic soil reaction $K_s$. For the simple geometry of a flexible tube surrounded symmetrically by a thick cylinder of sand and loaded by uniform, radially acting pressures (Fig. 1.1b), Luscher and Höeg (1964a) showed that $K_s$ backcalculated from experimental failure data was equivalent to the coefficient of resistance of the soil ring to uniform, outward acting pressure in the cavity. Thus $K_s$ was dependent upon the ring geometry and the "elastic" soil properties. Since these properties are not constants in a given soil but depend on the stress level and stress distribution, $K_s$ is affected not only by the pressure $p^*$ itself but also by the arching condition in the soil ring. Only for those combinations of soil and tube for which the arching effect is small can the modulus $K_s$ be expressed as a function of $p^*$ alone, then the buckling equation solved for $p^*$.

An equation of this kind was obtained by formulating

$$K_s = B\, E_s, \tag{3.3}$$

where $E_s$ = Young's modulus of the soil

---

2) Equations (3.1) and (3.2) were derived under the assumption that $n$ is an algebraic rather than an integer number. Consequently they do not give correct results for extremely low values of $K_s$ where $n$ is small. However, it can be shown that the error of Eq. (3.1) is practically negligible for $n \geq 3$.

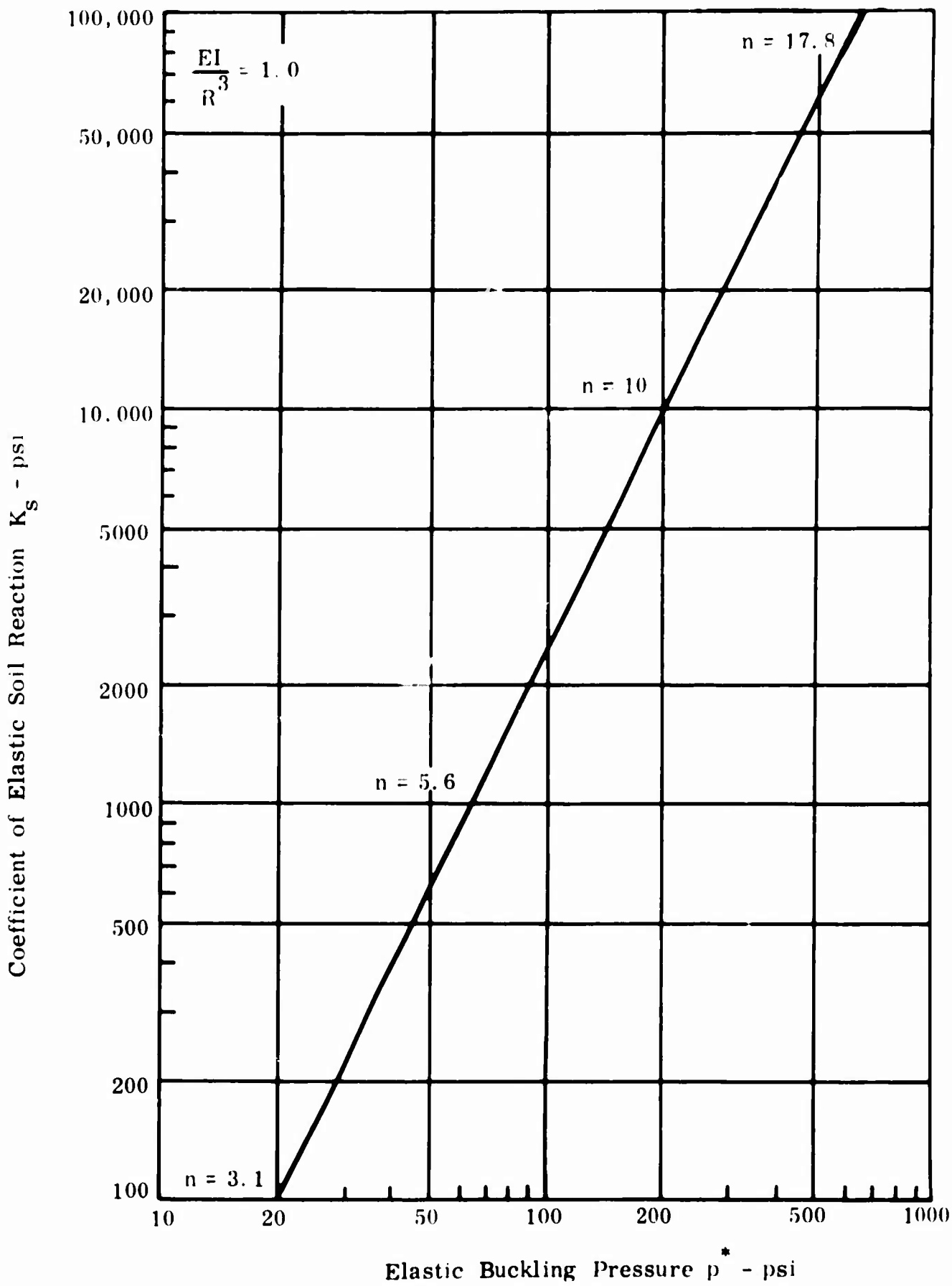


FIG. 3.1 THEORY FOR BUCKLING OF ELASTICALLY SUPPORTED RING

B = dimensionless coefficient dependent, for the assumed elastic ring, on the cylinder geometry and Poisson's ratio as shown in Fig. 3.2 [3)]

Replacing $E_s$ by 0.75 M, where M = constrained modulus of the soil (Luscher and Höeg, 1964a, p. 122), leads to the following alternate form of Eq. (3.3):

$$K_s = 0.75\ B\ M \tag{3.4}$$

The constrained modulus M of medium to dense Ottawa sand was determined in one-dimensional compression tests as $M = 1000\ p^{0.8}$. Substituting this expression into Eq. (3.4) and then Eq. (3.1), setting p = p* and solving for p* resulted in the buckling equation

$$p^* = 780 \left( \frac{EI\ B}{R^3} \right)^{5/6} \tag{3.5}$$

This expression correlated well with all buckling data involving only insignificant arching (see Figure 7.35 of Luscher and Höeg, 1964a).

The application of Eq. (3.5) to the failure conditions of smooth-walled tubes of different materials assumed symmetrically surrounded by the same soil with infinite thickness leads to the curves of Fig. 3.3. The figure demonstrates that the failure stress in the elastic range is controlled by buckling curves similar in nature to column buckling curves. At low slenderness ratios, these elastic buckling curves should be replaced by curves for inelastic buckling, which will be discussed in the next section. However, already the elastic buckling curves simply truncated by the horizontal yield stress line indicate, for various materials, the approximate magnitude of the critical diameter-to-thickness ratios at which the failure mode changes from compressive yield to buckling.

The information on the critical diameter-to-thickness ratios for

---

3) It should be noted that the definition of B is different from that used in Luscher and Höeg (1964a).

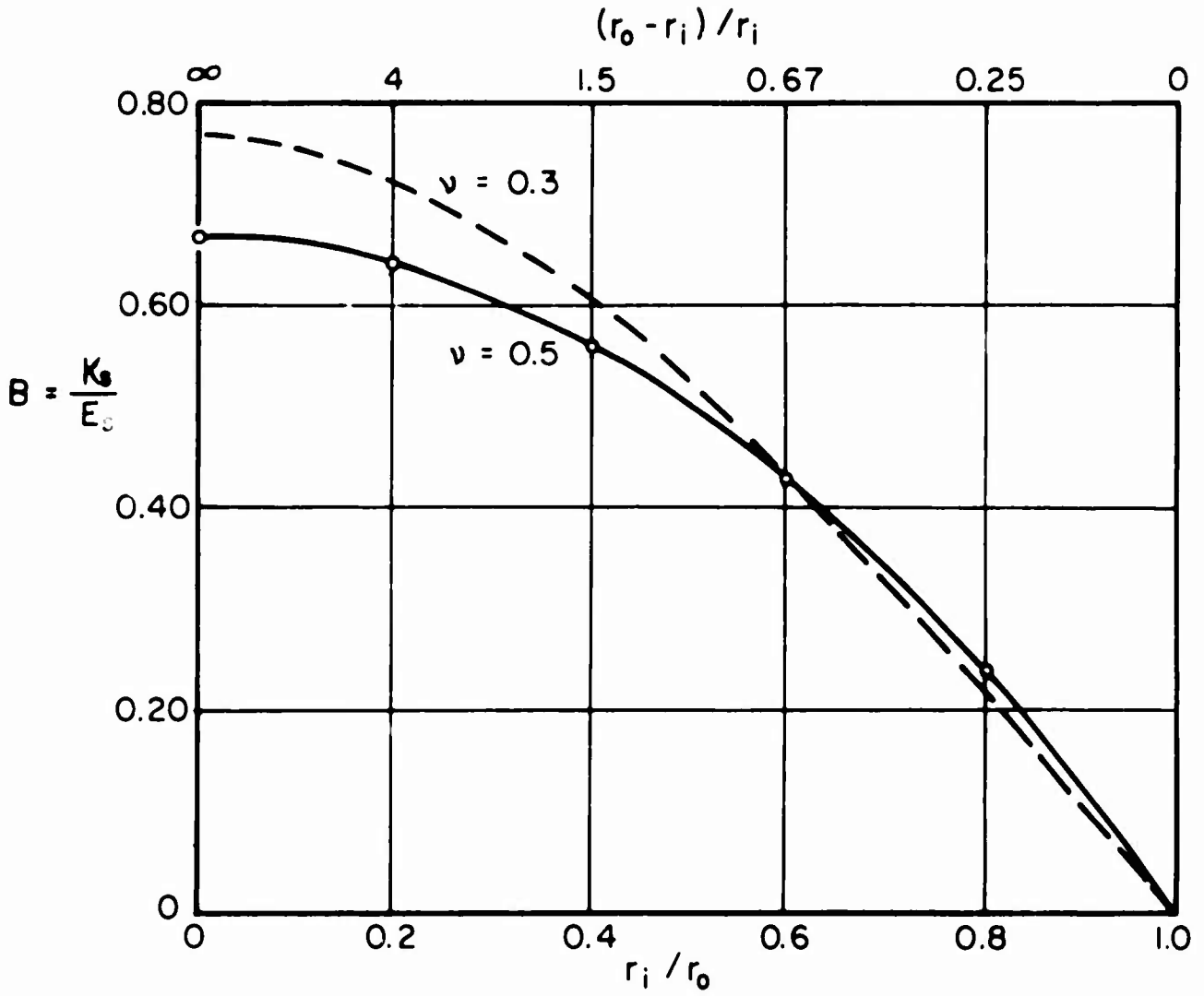


$$B = \frac{K_s}{E_s} = \frac{[1 - (r_i/r_o)^2]}{(1+\nu)\ [1+(r_i/r_o)^2\ (1-2\nu)]}$$

FIG. 3.2 COEFFICIENT OF ELASTIC SOIL REACTION FOR ELASTIC RING

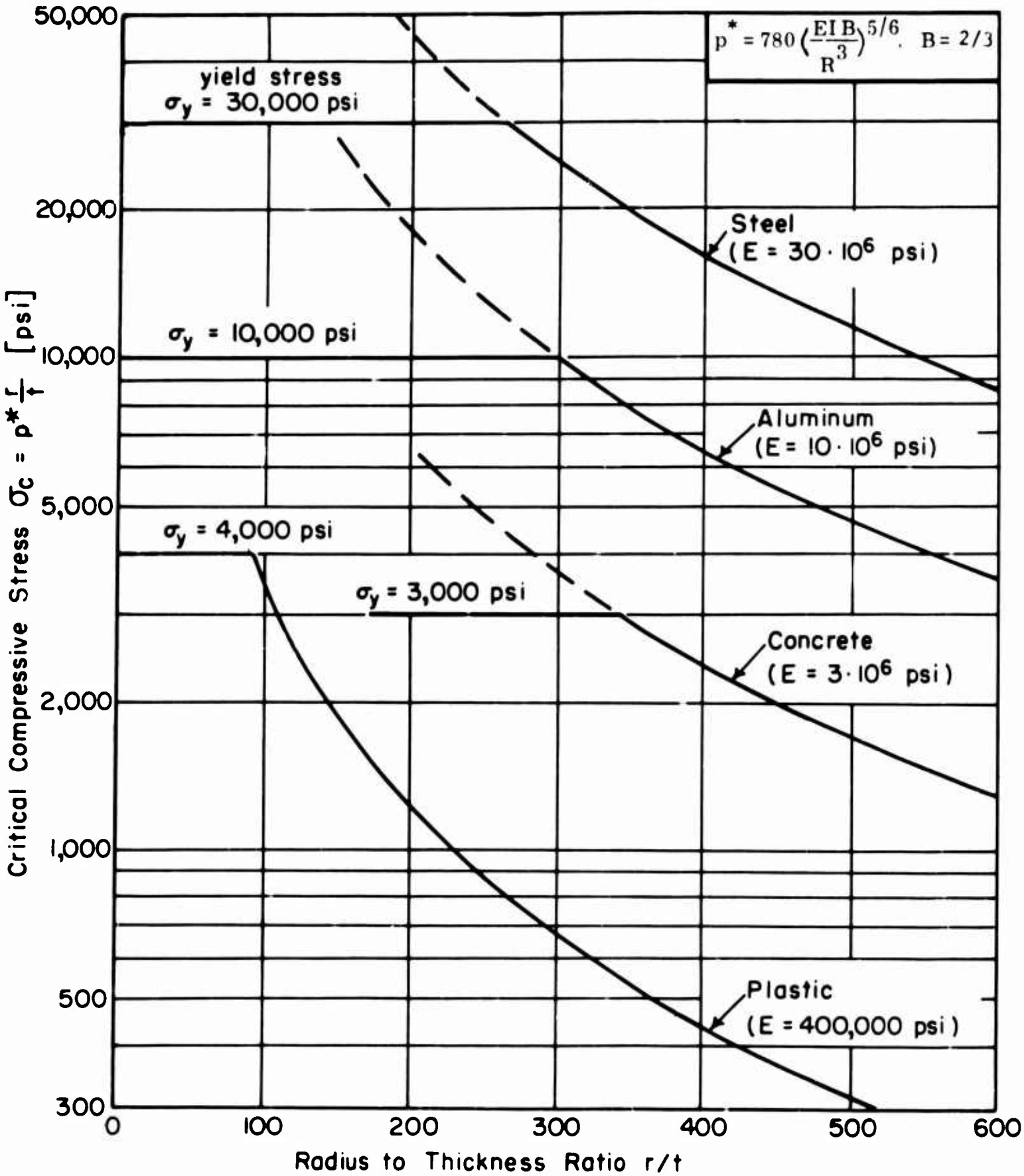


FIG. 3.3 BUCKLING STRENGTHS OF SOIL-SURROUNDED TUBES

Upper Limit

different materials is collected in Table 3.1, not only for the relationship of Eq. (3.5) but also for two similar relationships with reduced $K_s$ and therefore reduced buckling resistance, to investigate the effect of the quality of soil support. The specific reductions in $K_s$ are by factors of 5.3 and 16, those in p* by factors of 4 and 10. (The physical significance of these reductions is discussed in Section 3.7.) A tube designed with $D/t_{cr}$ has a critical failure pressure of just $p^*_{cr}$. If in a given case the applied pressure multiplied by the desired factor of safety is greater than $p^*_{cr}$, the required tube thickness will be larger than $t_{cr}$, therefore D/t will be smaller than $D/t_{cr}$, and design on the basis of yield stresses is permissible. If the design pressure is smaller than the critical buckling pressure $p^*_{cr}$, on the other hand, design on the basis of yield stresses (ring compression theory) is unsafe, since buckling rather than yielding will be the controlling failure mode. Moreover, the quoted critical radius-to-thickness ratios are upper limits, since inelastic buckling was neglected; this is discussed in Section 3.3. It is concluded from Table 3.1 that buckling will be the critical mode of failure in many situations involving smooth-walled, flexible tubes and should not be neglected in the design.

It should be noted at this time that the value for B is based on formulation of the resistance of an elastic thick ring to inside pressures uniformly applied, i.e., in a zero mode. Strictly speaking, the resistance to inside pressures with an $n^{th}$-mode distribution should be associated with buckling in the $n^{th}$ mode. This approach has been used by Forrestal and Herrmann(1964) to arrive at buckling pressures of a long cylindrical shell surrounded by an elastic medium. The resulting buckling resistances, for the case of $E/E_s = 10^3$ and $\nu = 0.3$, are higher than those calculated on the basis of Eq. (3.1) by factors 2.5 (at D/t = 100, n = 7) to 10 (at D/t = 1000, n = 70).

However, Eq. (3.5) and hence Eq. (3.4) have been verified by experiment. Furthermore, a relationship for $K_s$ derived by Meyerhof and Baikie (1963) on the basis of highly simplified concepts, and also verified by experiments, is practically identical to that of Fig. 3.2 for infinite soil thickness.

TABLE 3.1 INTERSECTION OF ELASTIC BUCKLING CURVE WITH YIELD STRESS LINE FOR VARIOUS MATERIALS AND SOIL STIFFNESSES

| Materiel | Material Properties | | Critical Buckling Condition Upper limit $E_s = 750\ p^{0.8}$ $p^* = 780\left(\frac{EIB}{R^3}\right)^{5/6}$ | | | Critical Buckling Condition Practical minimum $E_s = 140\ p^{0.8}$ $p^* = 195\left(\frac{EIB}{R^3}\right)^{5/6}$ | | | Critical Buckling Condition Lower limit $E_s = 47\ p^{0.8}$ $p^* = 78\left(\frac{EIB}{R^3}\right)^{5/6}$ | | |
|---|---|---|---|---|---|---|---|---|---|---|---|
| | E ksi | $\sigma_y$ ksi | $D/t_{cr}$ | $p^*_{cr}$ psi | $t_{cr}$ for D=10ft in. | $D/t_{cr}$ | $p^*_{cr}$ psi | $t_{cr}$ for D=10ft in. | $D/t_{cr}$ | $p^*_{cr}$ psi | $t_{cr}$ for D=10ft in. |
| High-str. steel | 30,000 | 70 | 300 | 466 | 0.40 | 120 | 1160 | 1.00 | 65 | 2150 | 1.85 |
| Mild steel | 30,000 | 30 | 530 | 113 | 0.23 | 212 | 282 | 0.58 | 114 | 530 | 1.05 |
| High-strength aluminum | 10,000 | 30 | 290 | 207 | 0.41 | 116 | 520 | 1.02 | 62 | 970 | 1.94 |
| Mild aluminum | 10,000 | 10 | 600 | 33 | 0.20 | 240 | 82 | 0.50 | 130 | 154 | 0.92 |
| Concrete | 3,000 | 3 | 680 | 9 | 0.18 | 272 | 22 | 0.45 | 146 | 41 | 0.82 |
| Typ. plastic | 400 | 4 | 190 | 42 | 0.63 | 76 | 105 | 1.60 | 40 | 200 | 3.00 |

1) Condition at which the failure mode changes from compressive yield to buckling.

The author's use in the theoretical derivation of a soil resistance based on a zero rather than an $n^{th}$ mode of deformation must be considered a deviation from rigorous theory. However, the theory agrees well with experimental evidence, and is on the conservative side of the rigorous theory while at the same time yielding theoretical buckling values much in excess of what had been considered possible heretofore. These facts make the theory an extremely useful tool, even if its derivation may include empirical steps.

## 3.3 INELASTIC BUCKLING OF SOIL-SURROUNDED, SMOOTH CYLINDERS

The curves shown in Fig. 3.3 represent the elastic buckling curves, which are similar in nature to Euler's curves for column buckling. Like the Euler curves, they are only valid in the elastic region and must be replaced by inelastic buckling curves for stresses approaching yield. How are these inelastic buckling curves obtained?

Based on Timoshenko and Gere (1961), Meyerhof and Baikie (1963) proposed use of the interaction formula

$$\frac{1}{\sigma_{cr}} = \frac{1}{\sigma_y} + \frac{1}{\sigma^*} \tag{3.6}$$

where $\sigma_{cr}$ = critical inelastic buckling stress

$\sigma_y$ = yield stress

$\sigma^*$ = $p^* R/t$, elastic buckling stress as discussed in the preceding section.

This equation allows for buckling in the inelastic region as well as accidental eccentricities and imperfections. Two examples of the resulting buckling curves, marked M + B, are shown in Fig. 3.4. Considering the ability of the soil to prevent buckling due to initial eccentricities, and the different character of stress-strain curves for different materials (e.g., steel and concrete), this formula appears too crude for general application, and is probably overconservative for many situations.

An alternate approach, commonly applied to column buckling, is

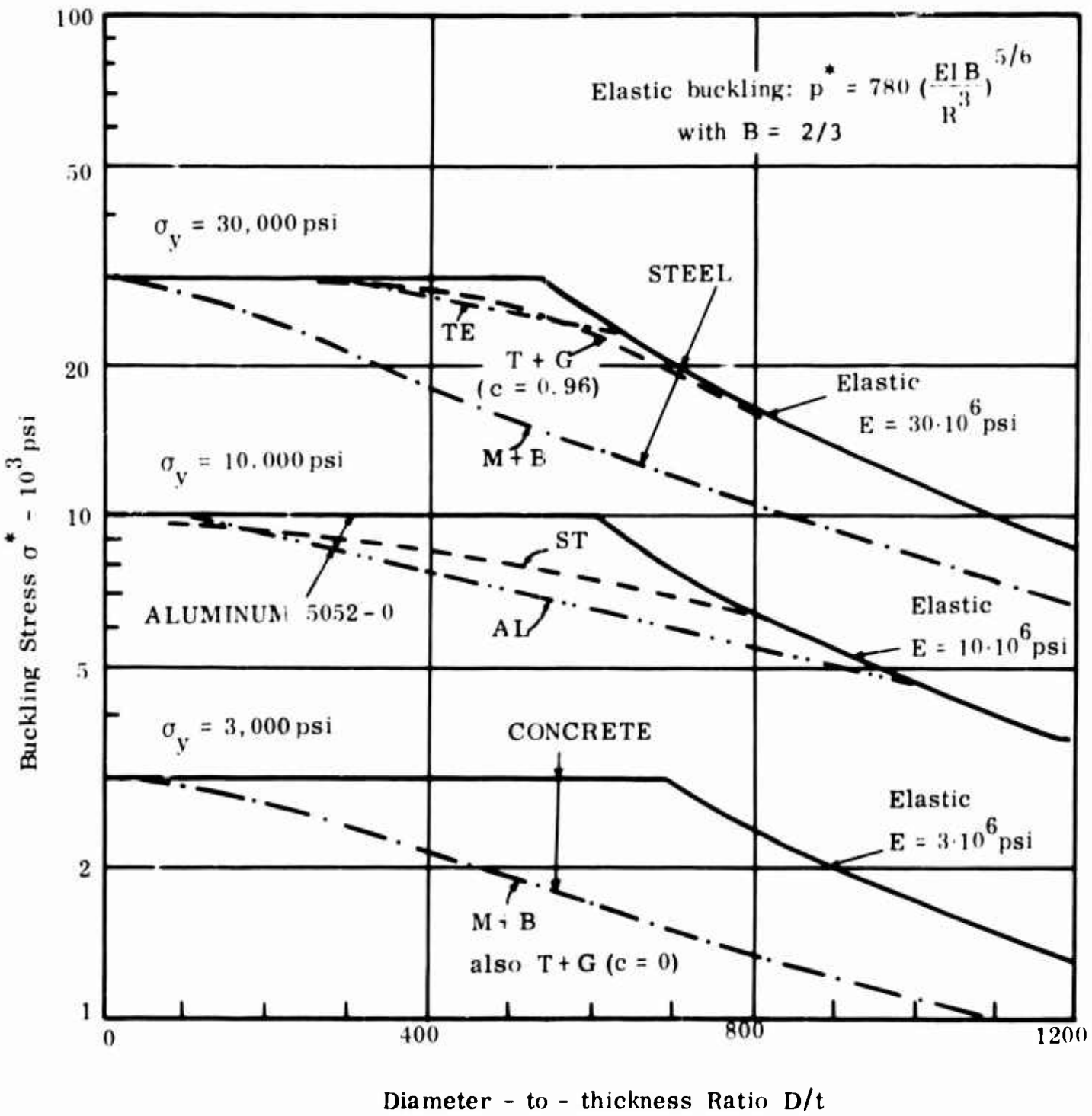


FIG. 3.4 INELASTIC BUCKLING CURVES

based on use of the tangent modulus at a given stress level in lieu of the modulus of elasticity in the buckling equation. The tangent modulus $E_t$ can be determined graphically from the stress-strain curves. Timoshenko and Gere (1961) recommend instead use of the equation

$$\frac{E_t}{E} = \frac{1 - \sigma/\sigma_y}{1 - c\,\sigma/\sigma_y},$$

where c is a coefficient depending upon the material. Nondimensional stress-strain curves for several values of c are shown in Fig. 3-19 of the reference. Use of this equation with the recommended values of c = 0.96 for steel and 0 for concrete resulted in the curves marked T + G in Fig. 3.4. Stüssi (1955) states that graphical determination of the tangent modulus is inaccurate, and recommends instead an iterative numerical procedure. His recursion formula applied to a typical stress-strain curve for aluminum 5052-0 yielded the curve marked ST in Fig. 3.4. The stress-strain curve would roughly correspond to a c of 0.85.

It is interesting to note at this point that the T + G curve for concrete with c = 0 coincides with Meyerhof's interaction curve for the same material. Thus Meyerhof's method corresponds in effect to the assumption of c = 0 for all materials and does not consider the different character of the stress-strain curves of different materials in the calculation of the buckling curve. It is felt that the methods which consider these differences by use of the tangent modulus in the buckling equation are superior.

Finally, inelastic tube buckling curves were calculated on the basis of column buckling curves. For Aluminum 5052-0, the ALCOA Handbook's straight-line inelastic column formula was transferred to Fig. 3.4 by plotting equal reductions from the elastic buckling stresses at equal slenderness ratios. (For example, if for a column with a slenderness ratio of 75 the elastic buckling formula yielded 18,200 psi, the plastic one 7,800 psi, and for the tube the elastic buckling stress was 18,200 psi at R/t = 200, then $\sigma_{cr}$ = 7800 psi at that R/t.) The resulting curve, marked AL in Fig. 3.4, is practically straight and represents an only

slightly conservative approximation to the curve based on the tangent modulus. By the same method, Tetmajer's straight line for steel (Timoshenko and Gere, 1961), modified to account for a lower yield stress, gave an inelastic buckling curve (marked TE in Fig. 3.4) very close to the curve calculated by the c-formula.

As protection against uncertainties in the soil support, a reasonably conservative choice of the soil modulus $K_s$ should be made (see Section 3.7). Then no additional conservative assumptions are required apart from any desired uniform factor of safety independent of D/t. Consequently it is recommended that an inelastic buckling curve based on the tangent modulus of the structural material be used.

An estimate can be made of the maximum amounts by which the inelastic buckling curves lie below a composite line formed by the elastic buckling curve and the horizontal yield stress line. This reduction is a function mainly of the stress-strain curve of the material. It is smallest for steel (15%), larger for aluminum (25%), largest for concrete (50%), among the materials investigated here. An empirically fitted relationship for the maximum reduction, which occurs at the intersection of the elastic buckling curve with the yield stress line, is

$$\sigma_{cr}/\sigma_y = 1 - 0.5\sqrt[3]{1-c} \quad . \qquad (3.7)$$

Knowing this point and the elastic buckling curve and yield stress line, which are both approached asymptotically, one can plot approximate inelastic buckling curves.

## 3.4 BUCKLING OF FULLY BURIED CYLINDERS

So far only buckling of a circular-symmetric tube-soil configuration has been considered. However, the situation of a buried cylinder (Fig. 1.1c), loaded either by a deep fill or by a surcharge applied at the soil surface, is not circular symmetric. The buried cylinder is deformed, with a horizontal diameter appreciably larger than the vertical diameter, and with soil

pressures not equal all around. These conditions may affect the buckling resistance. Further, arching and pressure redistribution have to be considered in the desired expression relating the critical surface pressure causing buckling to the pertinent parameters of the system. This section investigates the situation of "full" burial, i.e., a depth of cover of at least 1D (Höeg, 1965; Donnellan, 1964) where the effects of the soil boundary became negligible. The subsequent section investigates the effect of the depth of cover.

A first correction to be applied to the buckling equations, Eqs. (3.1) or (3.5), is one to account for pressure redistribution and arching. As concluded in Section 2.2, the pressure acting on the tube amounts to roughly two-thirds of the pressure applied on the surface of dense soil, and to the full value of the surface pressure for loose soil. Assuming now that the pressure causing buckling is unchanged from the circular-symmetric situation, the resulting equation for $p^*_o$, the surface pressure causing elastic buckling, is

$$p^*_o = 2\beta\sqrt{\frac{K_s EI}{R^3}} \quad , \tag{3.8}$$

where, as before, $\beta = 1.5$ for dense soil and 1.0 for loose soil. The same modification applies to Eq. (3.5) for dense Ottawa sand:

$$p^*_o = \beta \cdot 780 \left( \frac{EI\ B}{R^3} \right)^{5/6} \quad . \tag{3.9}$$

The second effect on buckling resistance to be investigated here is that of the deformation of the cylinder and the resulting non-uniformity of pressures acting on it. For purposes of this investigation, it is assumed that the buckling equations apply locally rather than for the tube as a whole, i.e., for local radii and local contact pressures. Further, it is assumed that the tube deforms according to the concepts outlined in Section 2.3 and that the deformations obey Eq. (2.3). Finally, it is

assumed that the hoop compressive resultant N equals $R\,p_o/\beta$ , the tube radius times the applied surface pressure modified by the arching factor $\beta$ , and that the local contact pressure can be computed as N divided by the local radius.

Under these assumptions, the crown and invert of the cylinder become the critical buckling locations. Substitution of expressions for the local radius and contact pressure at these locations into Eq. (3.9) and neglect of higher order terms leads to an expression for $p^*_e$, the surface pressure to buckle a deformed tube:

$$p^*_e = p^*_o \; (1 - 4.5\,\varepsilon_h), \tag{3.10}$$

Using Eq. (2.3) and neglecting the effect of the tube rigidity on deformation, this equation is transformed to

$$p^*_e = p^*_o \left(1 - \frac{3.5}{\beta}\,\frac{p^*_e}{E^*}\right) \quad . \tag{3.11}$$

Equations (3.10) and (3.11) express the dependency of the critical buckling pressure upon the tube deformation.

Two realistic expressions for E* can now be used to explore numerically the effect of $\varepsilon_h$ upon $p^*_e$. First, it is assumed that E* = 3000 psi, which is a reasonable value for a good backfill according to Section 2.3. Then,

$$p^*_e = p^*_o \; (1 - 0.0008\; p^*_e).$$

A second expression is the one backcalculated for laboratory-placed dense sand, $E^* = 2000\; p_e^{\frac{1}{2}}$. Then $E^*_{average} = 1000\; (p^*_e)^{\frac{1}{2}}$, and

$$p^*_e = p^*_o \; (1 - 0.00233\; (p^*_e)^{\frac{1}{2}}).$$

Typical values of reductions in buckling pressure obtained by the two

equations are the following:

| | $E^* = 3000$ psi | | $E^* = 2000\ p_o^{\frac{1}{2}}$ | |
|---|---|---|---|---|
| $p^*_o$ psi | $p^*_e$ psi | reduction % | $p^*_e$ psi | reduction % |
| 10 | 9.9 | 1 | 9.9 | 1 |
| 20 | 19.6 | 2 | 19.8 | 1 |
| 100 | 93 | 7 | 93 | 2 |
| 500 | 357 | 29 | 475 | 5 |

It is seen that the constant E*-value gives increasingly large reductions with increasing pressure level. In the case of the variable E*, the reduction increases more slowly with the pressure level, since now the deformation is proportional to only a fractional power of $p^*_e$. The result is more realistic for dense, i.e., locking sand.

The conclusion from the above is that deformation of the buried tube decreases the buckling resistance in dense soil inappreciably. Thus the buckling expressions, Eqs. (3.8) and (3.9), can in first approximation be directly applied to this situation. For loose backfill, however, for which the E* may be only a fraction of the 3000 psi assumed above, the effect of deformations can become appreciable. For instance, for the recommended maximum design deformation of 5% for buried cylinders (Spangler, 1960), which will ordinarily be reached only in loose soil, the reduction is 22%.

Experimental verification of these concepts is scarce, since the effect is always superimposed on, and is secondary to, the general increase in buckling resistance due to the surrounding soil. Further, the uncertainties in the amount of arching present are generally at least as large as the effect investigated here. For instance, the data by Luscher and Höeg (1964a), which were already quoted in support of arching concepts, allow conclusions supporting the concepts advanced here only if the arching concepts are assumed correct. Under this assumption the data indicate that for these tubes the reduction in buckling pressure due to deformation was negligible, as predicted by the theory for tubes buried in dense sand.

The conclusion, therefore, is that the main effects of burial to be considered are pressure redistribution and arching. The effect of deformations on buckling pressure can in general be neglected in view of the much larger uncertainties associated with the choice of the modulus of soil rigidity $K_s$. Equations (3.8) and (3.9) are the modified buckling equations to be used for buried cylinders.

## 3.5 BUCKLING OF SHALLOW-BURIED CYLINDERS

The preceding section explored the effect on buckling of burial at a depth of at least 1D, where the effects of the soil boundary become negligible. In this section the effect of a nearby boundary on the buckling resistance of a buried tube is to be investigated. The loading is applied as pressure on that boundary.

Three effects might tend to reduce the buckling resistance in this situation. The major one is a reduction in the coefficient of soil reaction $K_s$, which is responsible for the tremendous increase in buckling strength of a soil-surrounded tube over the unsupported tube. The second effect is an increase in deformation of the tube due to a loss in E* close to the surface. It is felt that this effect is much less important than the first one and can therefore be neglected. The same is true of the third effect, a possible reduction in arching and pressure redistribution with decreasing depth of cover. This effect is thought to be relatively small on the basis of the data collected in Section 2.2 and Höeg's (1965) and Donnellan's (1964) results.

Luscher and Höeg (1964a) have studied the variation of the coefficient of soil reaction $K_s$ with soil thickness for the circular-symmetric tube-soil configuration. They found that the coefficient B in Eq. (3.3) or (3.4), determined theoretically and plotted versus the ratio of the outside to the inside radius of the soil cylinder in Fig. 3.2, correctly described the variation for that case.

A conservative extension of this finding to the buried-cylinder situation is to use the cover over the crown as thickness of the equivalent

soil cylinder. In other words, Fig. 3.2, with the abscissa changed to $R/(d+R)$ (i.e., tube radius divided by depth of tube center), is directly applied to the buried-tube situation. This formulation is conservative because it uses as equivalent outside radius the shortest distance to the surface, which occurs at one point only. Ideally the average distance to the surface over a certain central angle, which might be related to the expected failure mode, should be chosen as outside radius. The need for such a modification is seen most clearly in tests where a tube with exposed crown still shows much higher buckling strength than an unsupported tube. For the sake of simplicity and conservatism, however, such a modification is not used here.

Two sets of failure data of tubes buried at shallow depth are available to check this theory. The first of these are the data from tests on two-ply aluminum foil tubes of 1.6-in. diameter buried in dense Ottawa sand, reported in Fig. 8.3 of Luscher and Höeg (1964a) and reproduced in Fig. 3.5 of this report. Also shown on the figure are the buckling pressures predicted by Eq. (3.9), with B from Fig. 3.2. The agreement between theory and experiment, particularly in regard to the variation of buckling pressure with depth, is seen to be satisfactory.

The second set of applicable data are found in Table 1 of Donnellan (1964) for buckling of shallow-buried aluminum cylinders of 4-in. diameter and D/t varying between 160 and 400. These data, together with theoretical predictions of buckling pressure, are given in Table 3.2. For the theoretical prediction, $E_s$ and therefore $K_s$ were assumed to be 25% higher than in the M.I.T. tests, since the E*-values backcalculated from tube deformation data (Table 2.2) were so related. Further, the buckling pressures in the inelastic range were determined from the available curve for Aluminum 5052-0 with a yield stress of 10,000 psi (Fig. 3.4), although the material of these tubes was Aluminum 2024-0 with a yield stress of only 8000 psi. Finally, the factor used to account for arching and pressure redistribution was not 1.5 as recommended in the preceding section but 2.0, in better agreement with factors actually observed in instrumented tests described in the same reference.

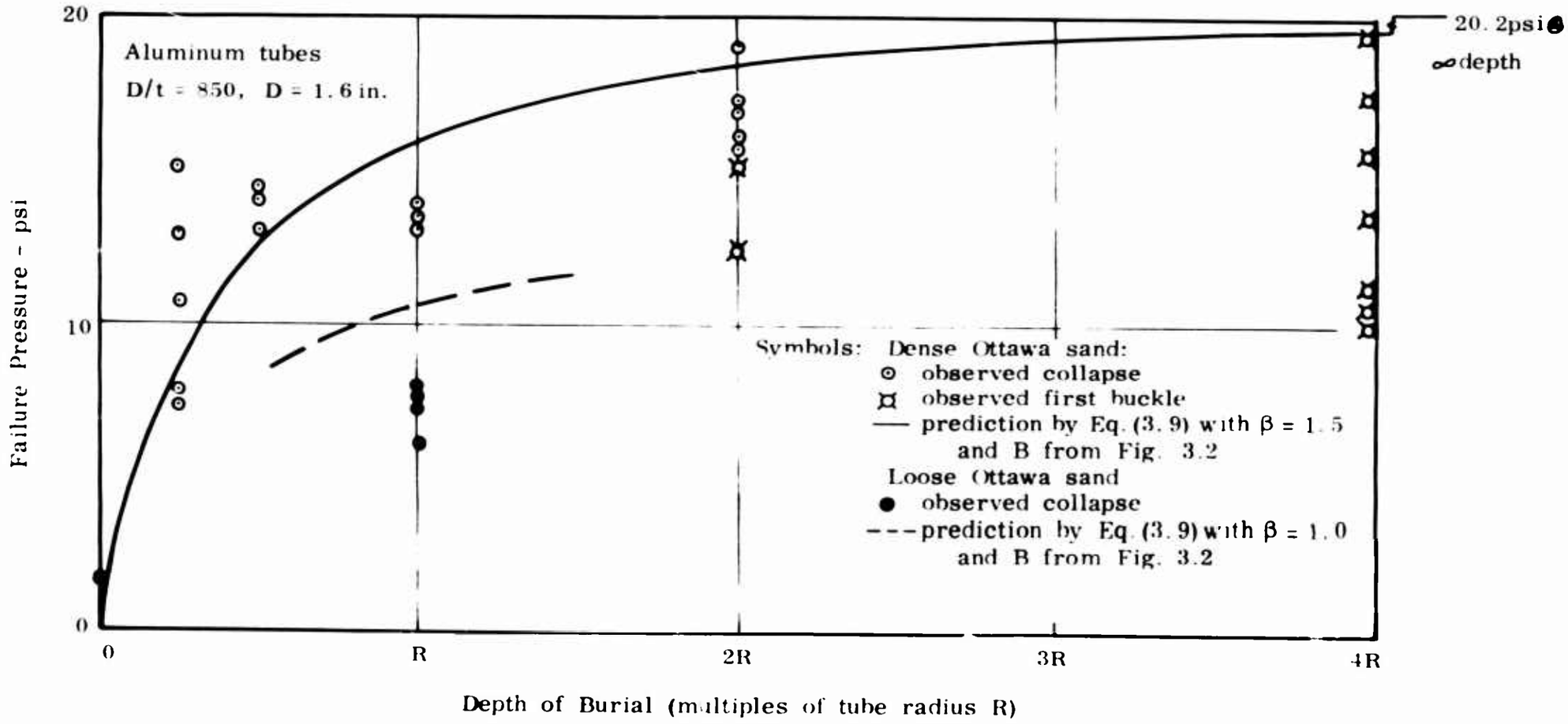


FIG. 3.5 CORRELATION OF M.I.T. TUBE BUCKLING DATA FOR SHALLOW DEPTH

TABLE 3.2 CORRELATION OF DONNELLAN'S DESTRUCTIVE TESTS

| | Experimental Collapse Pressure psi | | | | Theoretical Buckling Pressure psi | | | | |
|---|---|---|---|---|---|---|---|---|---|
| D/t | d/R = 0[1)] | 1/8 | 1/4 | 1/2 | d/R = 0 | 1/8 | 1/4 | 1/2 | ∞ |
| 400 | 12 | 42 | 90 | >150 | 0.3 | 55 | 74 | 86 | 89 |
| 333 | 18 | 84 | 152 | >150 | 0.6 | 80 | 96 | 106 | 109 |
| 250 | 28 | 133 | 137 | >150 | 1.4 | 123 | 138 | 147 | 151 |
| 200 | 40 | 140 | >150 | >150 | 2.8 | 168 | 180 | 188 | 192 |
| 160 | >150 | >150 | >150 | >150 | 5.4 | 220 | 231 | 240 | 245 |

1) d = depth of burial

The correlation observed in Table 3.2 is quite good, especially for the shallower depths of cover. For deeper depths, the theory underestimates the buckling strength, probably because of an underestimate of arching in this exceptionally dense sand. For zero depth, the buckling strength is much higher than for an unsupported tube for reasons given earlier. This case does not have much practical significance and is not covered by the theory.

It is concluded that the effect of depth of cover can be considered by varying the coefficient B in Eq. (3.9) according to Fig. 3.2, treating the depth like the thickness of a surrounding soil cylinder.

## 3.6 BUCKLING RESISTANCE OF CORRUGATED PIPES

Corrugation of pipes has been used for a long time as a means of increasing their flexural rigidity for handling, backfilling and better performance purposes. Since buckling has been found to be the controlling mode of failure for many smooth-walled cylinder installations, it appears of interest to investigate the buckling resistance of corrugated pipes.

The point of primary interest on the buckling curve is again the point of intersection with the yield-stress line. The "critical" diameter corresponding to this point has been calculated by Eq. (3.5) for two steel thicknesses, 10-gage (0.1345 in.) and 16-gage (0.0598 in.), and for different standard corrugations as well as for a smooth plate.[4] Additionally the critical diameter for a buckling curve that is lower by a factor 4 (i.e., $K_s$ reduced about five-fold) has been determined to investigate the effect of the quality of soil support. The results of these calculations are presented in Table 3.3.

---

[4] For simplicity, arching and pressure redistribution have been neglected in this calculation, as indicated by the use of Eq. (3.5) instead of (3.9). The conclusions will therefore be conservative for dense soil and about right for loose soil.

TABLE 3.3 BUCKLING RESISTANCE OF CORRUGATED PIPES

| Corrugation | $D_{cr}$ (in.) at Intersection of elastic buckling curve with yield stressline by Eq. (3.14) | | | |
|---|---|---|---|---|
| | Upper limit $p^* = 780 \left(\frac{EI\,B}{R^3}\right)^{5/6}$ | | Practical minimum $p^* = 195 \left(\frac{EI\,B}{R^3}\right)^{5/6}$ | |
| | 10-gage | 16-gage | 10-gage | 16-gage |
| Multi-plate 2 x 6 in. | 1500 | (1630) not used | 600 | (650) not used |
| Corrugation 1 x 3 in. | 700 | 760 | 280 | 300 |
| Corrugation $\frac{1}{2}$ x 2-2/3 in. | 340 | 370 | 134 | 150 |
| Smooth pipe[1)] | 80 | 38 | 32 | 14 |

1) These values are for 8- and 14-gage smooth pipes, which have about the same cross-sectional area as 10- and 16- gage corrugated pipes, respectively.

It is seen from the table that corrugation increases the critical diameter many-fold over that of a smooth tube of similar cross-sectional area. The increases are sufficient so that probably all critical diameters are beyond practically considered use, even in the case of the reduced soil support. It is therefore concluded that the ring compression theory, with some allowance for inelastic buckling at larger diameters, is valid for the large majority of corrugated pipes.

## 3.7 EFFECT OF SOIL STIFFNESS AND PORE PRESSURE ON TUBE BUCKLING RESISTANCE

### 3.7.1 Effect of Soil Stiffness

So far in this report Eqs. (3.5) and (3.9) have been used whenever numerical values of calculated buckling pressures were needed. The dependency of $K_s$ upon the confining pressure implied in these equations was experimentally determined in tube buckling tests. The dependency was also successfully related by theory to soil modulus values determined in one-dimensional compression tests. This correlation between $K_s$ and M allows investigation of the dependency of the buckling resistance upon the soil stiffness by use in the theory of constrained moduli for the soil of interest. Substituting Eq. (3.4), $K_s = 0.75\ B\ M$, into Eq. (3.8) leads to the controlling expression

$$p^*_o = 1.73\,\beta \sqrt{\frac{EI\ B}{R^3}}\ \sqrt{M}. \qquad (3.12)$$

The modulus M is usually determined in one-dimensional laboratory compression tests. An alternate way, for buried pipes, is to use M-values backcalculated from measured deformations of tubes (see Section 2.3, in particular Eq. (2.5)). This method may appear to be less direct, since M is related to E* by quite crude mathematics. However, for use in calculating $K_s$, which is a property of the soil next to the tube just like E* and hence closely related to E*, this method of determining M appears appropriate. The direct relationship between $K_s$ and E*, calculated for infinite depth from Eqs. (2.5) and (3.4) and Fig. 3.2, is

$$K_s = 2.5\ E^* \qquad (3.13)$$

Any error in this relationship should be systematic and subject to elimination by direct tests involving both properties.

Thus the task of choosing reasonable values of $K_s$ is reduced to the task of establishing reasonable values of M from one-dimensional compression tests, tube deformation data or tube buckling data. This is done with the help of Fig. 3.6, which is a summary plot of M-values from many sources. Whitman (1964) was particularly helpful in pointing out sources of compression test data. The M-values derived from tube deformation data were taken from Section 2.3. The following is concluded from the figure:

1. The M-curve backcalculated from tube buckling tests in dense sand (Luscher and Höeg, 1964a) represents a <u>reasonable upper limit</u> of the modulus. Higher values can be achieved particularly in the laboratory, but are probably unrealistic for practical situations. Thus Eqs. (3.5) and (3.9), which are based on this relationship, give reasonable upper limits of buckling resistance.

2. An M-curve 16 times lower than the upper limit gives a <u>reasonable lower limit</u> which should be conservative in most cases. The 16-fold reduction in M results in an approximately 10-fold reduction in $K_s$ (with the 5/6-power law used for p*). Lower limits may be expected for the one case of tubes driven or tunnelled into soft clay.

3. The "reasonable lower limit" of $K_s$ should never be reached for carefully installed pipes. A value of $K_s$ lowered by a factor of approximately five, giving a four-fold reduction in elastic buckling stress compared to the reasonable upper limit, appears to be a <u>reasonable practical minimum</u> for high-grade installations. This reduction has been used in the preceding sections as an example of reduced soil support.

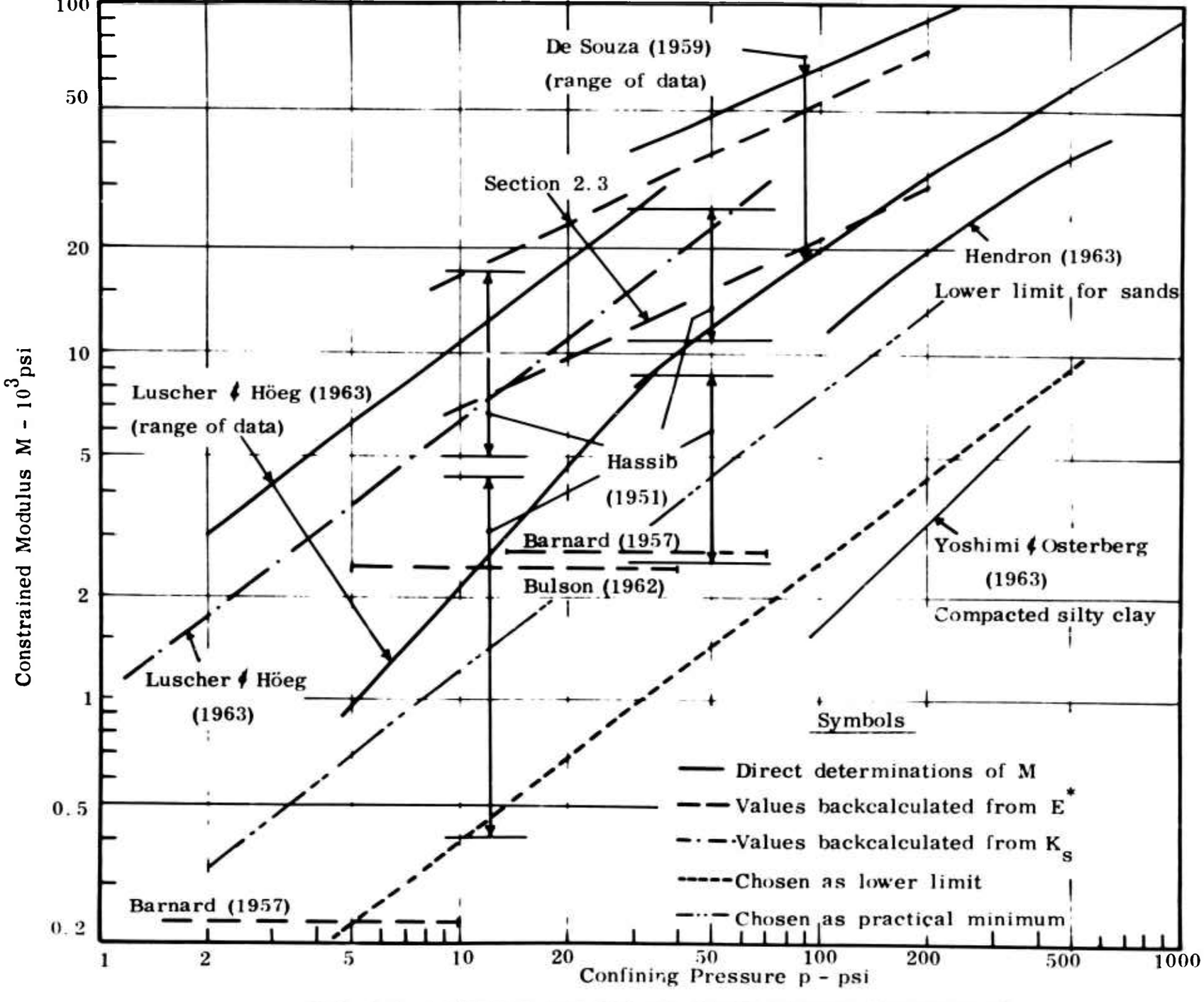


FIG. 3.6 LIMITING VALUES OF CONSTRAINED MODULUS M

The above information is summarized by the equation

$$p^*_o = A\,\beta\left(\frac{EI\,B}{R^3}\right)^{5/6} \qquad (3.14)$$

where A = 780 for "reasonable upper limit,"

A = 195 for "practical minimum,"

A = 78 for "reasonable lower limit."

Application of this equation to the "critical" buckling condition at which the failure mode changes from compressive yield to buckling is shown in Table 3.1. The critical diameter-to-thickness ratio is lowered by a factor 2.5 for the "practical minimum" compared to the upper limit of $K_s$. For the "reasonable lower limit" this reduction would be as high as 4.64-fold. Probably just the lowering of the ratio to the practical minimum, and certainly the lowering to the reasonable lower limit will bring most metallic tubes within the range where buckling rather than compressive yield is the controlling failure mode. This fact justifies and motivates adoption of corrugated cylinders for more efficient use of the structural material.

In practical cases, $K_s$ should be chosen on the basis of one-dimensional compression tests and substitution into Eq. (3.4). Alternatively, highly approximate values can be directly selected from the information presented in this report.

### 3.7.2 Effect of Pore Pressures

Another effect influencing the buckling resistance is the presence of pore pressure. This effect was studied by Luscher and Höeg (1964a) in tests in which part of the pressure acting on the tube was effective pressure $\bar{p}$ transmitted through the soil, and part was pore pressure u. The study established that only the effective stresses contributed to buckling resistance, while the neutral stresses contributed only to applied pressure. Thus the total pressure causing buckling can be formulated as

$$\bar{p} + u = 2\sqrt{\frac{K_s EI}{R^3}}\,, \qquad (3.15)$$

where now $K_s$ is a function of $\bar{p}$ only.

For the calculations exploring the effect of a given pore pressure, it is advantageous to work with a $K_s$ and consequently an M which are proportional to $\bar{p}$ rather than to the $(\bar{p})^{0.8}$ used to derive Eqs. (3.5) and (3.9). Formulating $M = m\,\bar{p}$, where m is the value of the M-function for $\bar{p}$ = 1 psi, and substituting into Eq. (3.15) results in

$$\bar{p} + u = 2\sqrt{\frac{EI\,B}{R^3}}\,\sqrt{m\,\bar{p}}\ .$$

Calling p* the solution which would be obtained for zero pore pressure,

$$p^* = \frac{4\,EI\,B\,m}{R^3}\ ,$$

the equation for the effect of u becomes

$$\bar{p} = \left[\frac{\sqrt{p^*}}{2} \pm \sqrt{\frac{p^*}{4} - u}\,\right]^2 \qquad (3.16)$$

Application of this equation leads to the interaction curves shown in Fig. 3.7.[5] It is seen that there are two possible failure conditions for each value of pore pressure, the lower one leading to a total buckling pressure $\bar{p} + u$ of less than 50 percent of the "dry buckling pressure" p*, the upper one to more than 50 percent. Which solution is controlling in a particular case will depend on the condition of loading. The lower part of the curve is valid in situations where the pore pressure is larger than half the total pressure, as is for instance the case in shallow tunnels under harbors and rivers. In protective construction, where pore pressures will generally be small or nonexistent, the upper part of the curve will apply. Consequently the reduction in total buckling pressure will remain

---

5) Strictly speaking, the curves for $(\bar{p} + u)/p^*$ and $u/p^*$ should not go to zero for $\bar{p}/p^* = 0$, but to the free-air (hydrostatic) buckling pressure. This limitation is the same as discussed in Footnote 2) in Section 3.2.

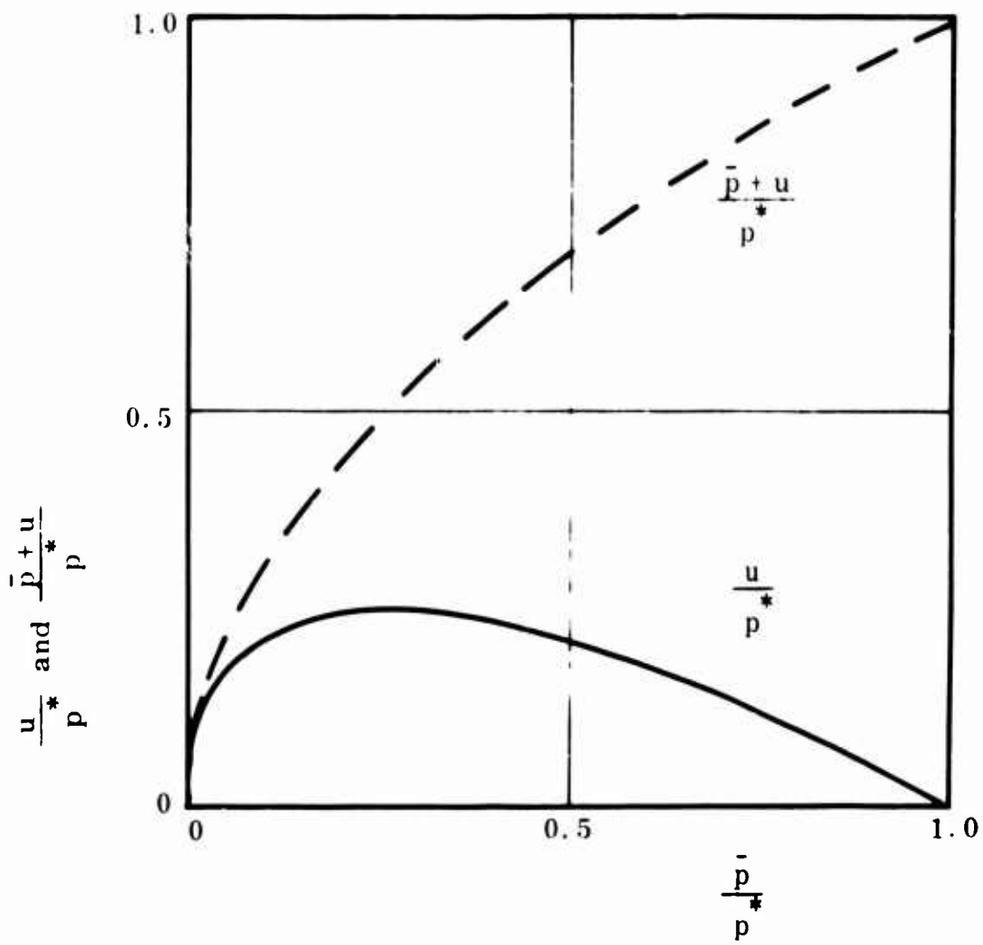


FIG. 3.7 EFFECT OF PORE PRESSURE ON BUCKLING RESISTANCE

less than 10 percent as long as the pore pressure is less than 10 percent of p*. The reduction reaches almost 30 percent for a pore pressure of 20 percent of p*, and is 50 percent for the maximum possible pore pressure of 25 percent of p*.

It is concluded that small pore pressures have relatively little effect upon buckling pressure as long as the effective stress is higher than the pore pressure, as is generally the case in protective construction. However, if the reverse is true, the tube buckling pressure can be reduced to a small fraction of the "dry buckling pressure" p*.

# CHAPTER 4

# SUMMARY AND CONCLUSIONS

## 4.1 SUMMARY

This report treats the "elastic" behavior and the failure condition of underground flexible cylinders. Specific aspects treated in Chapter 2 include the loads reaching the buried cylinders, the deformations undergone by the cylinder as the load is applied, and the possible failure modes. The most important conclusions were:

1. Arching was not found to be a very important factor for flexible cylindrical structures with horizontal axis buried in soil at depths up to several cylinder diameters. Active arching may reduce the load applied on cylinders buried in stiff soil by up to 30 or possibly 50 percent. Inversely, passive arching may subject cylinders buried in compressible soil to loads somewhat higher than applied on the soil surface. These relationships are expressed in the highly approximate equation

$$p = p_o/\beta \quad , \tag{2.1}$$

   where $\beta$ = 1.5 for stiff soil, 1.0 for compressible soil.

2. A modification of Spangler's classical equation for the calculation of pipe deformations is proposed, to take account of arching and to employ more realistic concepts of lateral pressures acting on the pipe:

$$\Delta \varepsilon_h = \Delta \frac{\Delta D_h}{D} = \frac{0.5/\beta \cdot p_o}{85\ EI/D^3 + 0.65\ E^*} \tag{2.3}$$

   Application of this equation in increments allows introduction of an E* that varies with pressure.

3. By use of Eq. (2.3) values of the modified modulus of passive soil resistance E* were backcalculated from available cylinder deformation data, and were correlated to constrained moduli M of the soils by the equation

$$E^* = 0.45\ M. \tag{2.5}$$

4. Compressive yield (or inelastic buckling at only slightly reduced pressure) is the desirable failure mode. To achieve it, the various modes of premature failure have to be avoided.

Buckling of underground flexible cylinders is treated extensively in Chapter 3, in continuation and termination of a study initiated several years ago. From the simple circular-symmetric situation analyzed earlier, the investigation was extended to underground geometry, to inelastic buckling, to corrugated pipes, and to the effects of soil stiffness and the presence of water. The main results were:

5. Theoretical equations for elastic buckling of the symmetric soil-tube configuration were established not only in terms of an unknown coefficient of soil reaction $K_s$ -

$$p^* = 2\sqrt{\frac{K_s EI}{R^3}} \tag{3.1}$$

- but also in terms of an experimentally determined dependency of $K_s$ upon the applied pressure, valid for dense sand:

$$p^* = 780\left(\frac{EI\ B}{R^3}\right)^{5/6} \tag{3.5}$$

Furthermore, $K_s$ was correlated to the one-dimensional soil modulus M:

$$K_s = 0.75\ B\ M\ , \tag{3.4}$$

where B is a coefficient obtained from Fig. 3.2.

6. The buckling theory was extended to the inelastic range by use of the tangent modulus of the structural material in the buckling equations. A procedure was proposed for simple determination of an approximate inelastic buckling curve, fitted between the horizontal yield stress line on one side and the elastic buckling curve on the other side.

7. The effect of burial was considered by including in the buckling equations a factor $\beta$ to account for arching, and by using the theoretical dependency (expressed in Fig. 3.2) of $K_s$ upon the soil cover over the cylinder:

$$p^*_o = 2\beta\sqrt{\frac{K_s\ EI}{R^3}} \tag{3.8}$$

$$p^*_o = 780\beta\left(\frac{EI\ B}{R^3}\right)^{5/6} \tag{3.9}$$

The effect of tube deformations upon buckling was found to be relatively minor.

8. While for many smooth-walled, flexible metallic tubes elastic buckling is the controlling mode of failure, corrugation increases the buckling resistance to a point where inelastic buckling or compressive yield usually are the controlling failure modes.

9. The effect of soil stiffness was considered by establishing a reasonable range of possible values of $K_s$. Use of the correlation between $K_s$ and M, as well as the correlation between E* and M, resulted in the buckling expression

$$p^*_o = A\beta\left(\frac{EI\ B}{R^3}\right)^{5/6} \tag{3.14}$$

where A = 780 for "reasonable upper limit,"
A = 195 for "practical minimum,"
A = 78 for "reasonable lower limit."

10. The presence of pore pressure reduces the buckling resistance only inappreciably, as long as the pore pressure is considerably smaller than the effective stress.

## 4.2 CONCLUSIONS REGARDING THE IMPORTANCE OF TUBE BUCKLING

When good backfill procedures are used, the expected critical D/t-ratios at which the failure mode changes from compressive yield to buckling are as given in Table 3.1 under "practical minimum." The quoted values place many smooth metallic tubes into the region where buckling failure is controlling, and where consequently the buckling theory presented in this report should be applied. Further, even if D/t is only approaching the critical value, inelastic buckling and the effect of tube deformations reduce the critical pressure below yield. This, and the uncertainty associated with arching, forbid use of the full yield stress in design even below the critical D/t. For D/t above the critical value, the buckling pressure approaches asymptotically the calculated elastic buckling stress.

Corrugation of the cylinder material is an extremely effective means of increasing the buckling resistance, so that elastic buckling should only in extreme cases be controlling. The knowledge of how close one is to the critical condition in a given situation is helpful in evaluating the required factor of safety with respect to yield.

The correlation of $K_s$ with M or E*, and the methods of determining $K_s$ from one-dimensional compression tests or from the information presented herein, can presently be considered only rough approximations. Hopefully, more data will soon become available to improve the method of selecting $K_s$ for a given situation.

## REFERENCES


Allgood, J. R. (1965) The Behavior of Shallow-Buried Cylinders - A Synthesis and Extension of Contemporary Knowledge, Technical Report R 344 of the U. S. Naval Civil Engineering Laboratory. Also in Proceedings of the Symposium on Soil-Structure Interaction, Tucson, Arizona, Sept. 1964.

ASCE (1964) "Development and Use of the Modpares Device," Research Council on Pipeline Crossings of Railroads and Highways, Proc. ASCE, Vol. 90, No. PL1, Jan.

Barnard, R. E. (1957) "Design and Deflection Control of Buried Steel Pipe Supporting Earth Loads and Live Loads," Proceedings of the ASTM, Vol. 57, pp. 1233-1256.

Bulson, P. S. (1962) Deflection and Collapse of Buried Tubes, Report RES 7/1 of the Military Engineering Experimental Establishment (MEXE), England.

Demmin, J. (1964) Field Verification of Ring Compression Conduit Design, Report of Armco-Thyssen, Dinslaken, Germany.

de Souza, J. M. (1959) Compressibility of Quartz Sand at High Pressure, S. M. Thesis, M.I.T. Department of Civil Engineering.

Donnellan, B. A. (1964) The Response of Buried Cylinders to Quasi-Static Overpressures, Report No. AFWL TDR-64-13. Also in Proceedings of the Symposium on Soil-Structure Interaction, Tucson, Arizona, Sept. 1964.

Finn, W. D. L. (1963) "Boundary Value Problems of Soil Mechanics," Proceedings ASCE, Vol. 89, No. SM5, Sept.

Forrestal, M. J., and G. Herrmann (1964) "Buckling of a Long Cylindrical Shell Surrounded by an Elastic Medium," ASCE Structural Engineering Conference and Annual Meeting, October, Conference Preprint 108.

Hassib, (1951) Consolidation Characteristics of Granular Soils, Columbia University, New York.

Hendron, A. J. (1963) The Behavior of Sand in One-Dimensional Compression, Report No. AFWL TDR-63-3089. Also Ph.D. Thesis, University of Illinois Dept. of Civil Engineering.

Höeg, K. (1965) Pressure Distribution on Underground Structural Cylinders, Report No. AFWL TR 65-98.

Lambe, T. W. (1960) Buried Flexible Pipes, Report for the Algonquin Gas Transmission Company, Boston, Mass.

Lambe, T. W. (1963) "An Earth Dam for the Storage of Fuel Oil," 2nd Pan-American Conference on Soil Mechanics and Foundation Engineering, Brazil.

Link, H. (1963) "Beitrag zum Knickproblem des elastisch gebetteten Kreisbogenträgers," Stahlbau, Vol. 32, No. 7, July, pp. 199-203.

Luscher, U. (1963) Study of the Collapse of Small Soil-Surrounded Tubes, Report No. AFSWC TDR-63-6.

Luscher, U., and K. Höeg (1964a) The Interaction Between a Structural Tube and the Surrounding Soil, Technical Documentary Report No. AFWL TDR-63-3109.

Luscher, U., and K. Höeg (1964b) "The Beneficial Action of the Surrounding Soil on the Load-Carrying Capacity of Buried Tubes," Proceedings of the Symposium on Soil-Structure Interaction, Tucson, Arizona, September, pp. 393-402. Also M.I.T. Civil Engineering Department Professional Paper No. P64-24, May 1964.

Luscher, U., (1965) Static and Dynamic Tests on 4-Inch-Diameter Cylinders, Report No. AFWL TDR 64-92, in preparation.

Marino, R. L., Jr., (1963) A Study of Static and Dynamic Resistance and Behavior of Structural Elements, Report No. AFWL TDR-63-3060.

Meyerhof, G. G., and L. D. Baikie (1963) "Strength of Steel Culvert Sheets Bearing Against Compacted Sand Backfill," Highway Research Board Record No. 30, pp. 1-14.

Newmark, N. M. and J. D. Haltiwanger (1962) Air Force Design Manual, Report No. AFSWC TDR-62-138 (confidential).

Robinson, R. R., (1962) The Investigation of Silo and Tunnel Linings, Report No. AFSWC TDR-62-1.

Spangler, M. G., (1960) Soil Mechanics, Int. Textbook Co.

Stüssi, F., (1955) Tragwerke aus Aluminium, Springer-Verlag.

Timoshenko, S., and J. Gere (1961) Theory of Elastic Stability, McGraw-Hill.

Watkins, R. K., (1959) "Influence of Soil Characteristics on the Deformation of Embedded Flexible Pipe Culverts," Highway Research Board Bulletin 223, pp. 14-24.

White, H. L., (1961) "Largest Metal Culvert Designed by Ring Compression Theory," Civil Engineering, Vol. 31, January, pp. 52-55.

White, H. L., and J. P. Layer (1960) "The Corrugated Metal Conduit as a Compression Ring," Highway Research Board Proc.

Whitman, R. V., (1964) "Mechanical Properties of Soil," Nuclear Geoplosics, Part Two - Mechanical Properties of Earth Materials, DASA-1285 (II).

Whitman, R. V., and U. Luscher (1962) "Basic Experiment Into Soil-Structure Interaction," Proc. ASCE, Vol. 88, No. SM6, Dec.

Whitman, R. V., U. Luscher, and A. R. Philippe (1961) Preliminary Design Study for a Dynamic Soil Testing Laboratory, Final Report for Contract AF 29(601)-1947. Report No. AFSWC TR-61-58 contains Appendices K, L, M and N to this report.

Yoshimi, Y., and J. O Osterberg (1963) "Compression of Partially Saturated Cohesive Soils," Proc. ASCE, Vol. 89, No. SM4, July.

BLANK PAGE

UNCLASSIFIED
Security Classification

## DOCUMENT CONTROL DATA - R&D

*(Security classification of title, body of abstract and indexing annotation must be entered when the overall report is classified)*

1 ORIGINATING ACTIVITY *(Corporate author)*
Massachusetts Institute of Technology, Department of Civil Engineering
Cambridge 39, Massachusetts

2a REPORT SECURITY CLASSIFICATION
UNCLASSIFIED

2b GROUP

3 REPORT TITLE
BEHAVIOR OF FLEXIBLE UNDERGROUND CYLINDERS

4 DESCRIPTIVE NOTES *(Type of report and inclusive dates)*
1 March 1964-2 April 1965

5 AUTHOR(S) *(Last name, first name, initial)*
Luscher, Ulrich

6 REPORT DATE
September 1965

7a TOTAL NO. OF PAGES
74

7b NO. OF REFS
33

8a CONTRACT OR GRANT NO. AF 29(601)-6368

b. PROJECT NO. 5710

c. DASA Subtask No. 13.157

d

9a ORIGINATOR'S REPORT NUMBER(S)
AFWL-TR-65-99

9b OTHER REPORT NO(S) *(Any other numbers that may be assigned this report)*

10 AVAILABILITY/LIMITATION NOTICES
DDC release to OTS is authorized.

11 SUPPLEMENTARY NOTES

12 SPONSORING MILITARY ACTIVITY
AFWL (WLDC)
Kirtland AFB, NM 87117

13 ABSTRACT An investigation was made of the "elastic" behavior and failure condition of underground flexible cylinders with particular attention given to arching, deformation and buckling. The report presents no new data, rather draws heavily from experimental and theoretical work done in the past several years in an attempt to arrive at a unified picture of the chosen aspects of behavior. Active arching was found to reduce the load acting on tubes buried at depths up to several diameters in stiff soil by an average of 30 percent. On the other hand, passive arching may subject tubes buried in compressible soil to loads somewhat higher than applied on the surface. Spangler's deformation equation was modified to account for arching, lateral pressures, and variability of the soil modulus with pressure. Values of the modified modulus of passive soil resistance, backcalculated by the new equation from tube deformation data, were successfully related to the constrained modulus of the soil. A comprehensive theory of buckling of underground cylinders is presented. It starts with the previously derived theory for elastic buckling in the circular-symmetric tube-soil configuration and extends it to cover (1) elastic buckling of an underground cylinder; (2) inelastic buckling; (3) the effects of soil stiffness and presence of water; and (4) buckling of corrugated cylinders. It proved possible to correlate the soil modulus $K_s$ controlling buckling to the constrained modulus M of the soil. The theory agreed well with the few available data. More comparisons with laboratory and field data are required, in particular to verify the values of $K_s$ and their relationship to values of M. Regardless of the exact value of $K_s$, however, it was shown that for many practical situations of underground cylinders the controlling mode of failure is buckling rather than compressive yield.

DD FORM 1 JAN 64 1473

UNCLASSIFIED
Security Classification

| 14 KEY WORDS | LINK A ROLE | LINK A WT | LINK B ROLE | LINK B WT | LINK C ROLE | LINK C WT |
|---|---|---|---|---|---|---|
| Behavior of flexible pipe | | | | | | |
| Buried cylinder research | | | | | | |
| Soil-structure interaction | | | | | | |
| Horizontally buried cylinders | | | | | | |

## INSTRUCTIONS

1. ORIGINATING ACTIVITY: Enter the name and address of the contractor, subcontractor, grantee, Department of Defense activity or other organization *(corporate author)* issuing the report.

2a. REPORT SECURITY CLASSIFICATION: Enter the overall security classification of the report. Indicate whether "Restricted Data" is included. Marking is to be in accordance with appropriate security regulations.

2b. GROUP: Automatic downgrading is specified in DoD Directive 5200.10 and Armed Forces Industrial Manual. Enter the group number. Also, when applicable, show that optional markings have been used for Group 3 and Group 4 as authorized.

3. REPORT TITLE: Enter the complete report title in all capital letters. Titles in all cases should be unclassified. If a meaningful title cannot be selected without classification, show title classification in all capitals in parenthesis immediately following the title.

4. DESCRIPTIVE NOTES: If appropriate, enter the type of report, e.g., interim, progress, summary, annual, or final. Give the inclusive dates when a specific reporting period is covered.

5. AUTHOR(S): Enter the name(s) of author(s) as shown on or in the report. Enter last name, first name, middle initial. If military, show rank and branch of service. The name of the principal author is an absolute minimum requirement.

6. REPORT DATE: Enter the date of the report as day, month, year, or month, year. If more than one date appears on the report, use date of publication.

7a. TOTAL NUMBER OF PAGES: The total page count should follow normal pagination procedures, i.e., enter the number of pages containing information.

7b. NUMBER OF REFERENCES: Enter the total number of references cited in the report.

8a. CONTRACT OR GRANT NUMBER: If appropriate, enter the applicable number of the contract or grant under which the report was written.

8b, 8c, & 8d. PROJECT NUMBER: Enter the appropriate military department identification, such as project number, subproject number, system numbers, task number, etc.

9a. ORIGINATOR'S REPORT NUMBER(S): Enter the official report number by which the document will be identified and controlled by the originating activity. This number must be unique to this report.

9b. OTHER REPORT NUMBER(S): If the report has been assigned any other report numbers *(either by the originator or by the sponsor)*, also enter this number(s).

10. AVAILABILITY/LIMITATION NOTICES: Enter any limitations on further dissemination of the report, other than those imposed by security classification, using standard statements such as:

(1) "Qualified requesters may obtain copies of this report from DDC."

(2) "Foreign announcement and dissemination of this report by DDC is not authorized."

(3) "U. S. Government agencies may obtain copies of this report directly from DDC. Other qualified DDC users shall request through _____."

(4) "U. S. military agencies may obtain copies of this report directly from DDC. Other qualified users shall request through _____."

(5) "All distribution of this report is controlled. Qualified DDC users shall request through _____."

If the report has been furnished to the Office of Technical Services, Department of Commerce, for sale to the public, indicate this fact and enter the price, if known.

11. SUPPLEMENTARY NOTES: Use for additional explanatory notes.

12. SPONSORING MILITARY ACTIVITY: Enter the name of the departmental project office or laboratory sponsoring *(paying for)* the research and development. Include address.

13. ABSTRACT: Enter an abstract giving a brief and factual summary of the document indicative of the report, even though it may also appear elsewhere in the body of the technical report. If additional space is required, a continuation sheet shall be attached.

It is highly desirable that the abstract of classified reports be unclassified. Each paragraph of the abstract shall end with an indication of the military security classification of the information in the paragraph, represented as *(TS)*, *(S)*, *(C)*, or *(U)*.

There is no limitation on the length of the abstract. However, the suggested length is from 150 to 225 words.

14. KEY WORDS: Key words are technically meaningful terms or short phrases that characterize a report and may be used as index entries for cataloging the report. Key words must be selected so that no security classification is required. Identifiers, such as equipment model designation, trade name, military project code name, geographic location, may be used as key words but will be followed by an indication of technical context. The assignment of links, rules, and weights is optional.